ANNALS OF GEOPHYSICS, 68, 6, EP687, 2025; doi:10.4401/ag-9455
OPEN ACCESS

Predict part 2: Building a Geo-Database and a 3D subsurface model for the historical center of Rome

Daniele Silvestri*,[1], Paola Bordoni[2], Daniela Famiani[2], Fabrizio Marra[2], Carlo Rosa[3], Riccardo Salvini[1]

(1) University of Siena, Department of Physical Sciences, Earth and Environment, Siena, Italy
(2) Istituto Nazionale di Geofisica e Vulcanologia, Rome, Italy
(3) SIGEA Lazio-APS, Rome, Italy

Article history: received October 14, 2025; accepted October 30, 2025

Abstract

In many countries, the subsurface is increasingly recognized as an integral part to urban planning, requiring detailed knowledge of the 3D subsurface geometry and properties of both natural sediments and artificial deposits. The underground data are essential for visualizing and analyzing geological features in combination with artificial structures, assessing risks related to groundwater protection, seismic hazard, and preserving archaeological heritage. Geographic information systems offer powerful tools for managing and visualizing spatial data, facilitating the creation of detailed subsurface models. In this work, a novel geo-lithologic database has been implemented in a GIS environment to provide a comprehensive understanding of the subsurface of the Roman urban area. The Roman area, despite being located in a moderate seismic hazard zone, is exposed to a significant level of seismic risk, also due to the unique cultural heritage of its historical center. Over 800 boreholes, with average depths of 50-60 m, were georeferenced and interpreted from a large database of civil engineering boreholes. This geodatabase (hereafter GDB) served as the basis for developing a 3D subsurface model, finalised to seismic response analyses in the framework of the INGV Dynamic Planet ST-Predict project. In addition, the development of an implicit 3D geological model for Rome, based on stratigraphic correlations and lithofacies analysis, provides crucial input for future analyses on the Quaternary deposits of the Roman area.

Keywords: Geology of Rome; 3D geological modeling; Borehole; Implicit model; Quaternary

1. Introduction

Three-dimensional geological models in GIS (Geographic Information System) environment have revolutionized Earth Science by enabling the integration of disparate datasets into a single spatial framework (Ford et al., 2010, Le Yu et al., 2008; Von der Taan et al., 2019). This allows for a more comprehensive understanding of subsurface structures and their relationships (Zhang and Xiao, 2013). By moving beyond traditional 2D representations, 3D modeling enhances visualization and analysis, leading to improved decision-making in various geological applications (Terrington et al., 2008). Integrating borehole data with geophysical surveys is crucial for urban geoscience projects to constrain models and accurately reproduce data. This combination provides a more complete understanding of subsurface conditions, essential for informed decision-making in urban planning and resource management (Giacomelli et al., 2023). This study is part of risk-prevention measures aimed at reducing the impact of future disasters on cities and their cultural heritage. Downtown Rome contains a unique and fragile cultural heritage of outstanding value (Di Salvo et al., 2020). Although the area is classified as having moderate seismic hazard (Bonilla et al., 2011; Martino et al., 2015; Stucchi et al., 2011), the seismic risk remains considerable because of the high exposure of population, infrastructure, and cultural heritage. Among all its applications, geological model presented here has been developed as part of the activities of Work Package 1 within the project

"Seismic response in downtown Rome from new strong motion observations and 1D to 3D seismic wave propagation modeling" (acronym: ST-Predict). The project is funded under the INGV initiative *Dynamic Planet-Working Earth* (https://progetti.ingv.it/it/pian-din). In fact, an accurate reconstruction of the 3D geometry of the subsurface geology is essential to study its influence on seismic wave propagation.

Creating a reliable and useful urban subsurface model often requires the integration of information from multiple organisations and databases. To construct the model, it is necessary to combine different types of data. The spatial density of the data is typically variable, and, more importantly, the data formats may be heterogeneous, making interoperability difficult. Therefore, it is necessary to collect, validate, and store the entire dataset in a unified spatial database to establish the stratigraphy and relevant properties of the soil beneath a specific site. In the past, geologists have solved practical problems using 2D geological maps and cross-sections, geotechnical and geophysical survey records, borehole logs. To enhance the accuracy of geological analysis and engineering design, it is necessary to construct reliable 3D models that integrate original field data from the database and clearly define the stratigraphic (and tectonic) boundaries. This approach provides a more comprehensive understanding of the soil deposits. GIS have the advantage of integrating spatial analysis, a database management system that includes geographic attributes, and graphic visualization capabilities. It is defined as a powerful set of tools for collecting, storing, retrieving, transforming, and displaying spatial data from the real world (Burrough et al., 2015). It also facilitates spatial searches and overlays based on user-defined functions for generating new datasets and models. Therefore, a GIS was adopted to manage the spatially variable geological data and address the associated spatial complexity.

The added value of this study consists of the implementation of an implicit 3D geological model of the historical center of Rome, aimed at advancing the assessment of seismic risk in a densely built and culturally invaluable urban environment. The central research question addressed is how implicit 3D modeling can enhance the representation of stratigraphic and structural heterogeneities, thereby providing more robust input for seismic hazard and risk analyses. The proposed workflow is articulated into four main phases.

The initial phase focused on the stratigraphic interpretation of borehole data to establish a robust geological framework, based on an extensive drilling dataset which represents a unique feature in this urban context, providing a comprehensive and detailed view of the geological subsurface of Rome (Vergari et al., 2020).

In the second phase, a Geo-lithological DataBase (GDB) was implemented in a GIS environment to provide a comprehensive understanding of the subsurface of the Roman area, including the visualization of stratigraphic features and the identification of layer boundaries. Starting from the creation of the GDB in a GIS environment, information concerning more than 800 boreholes, with average depths of 50-60 m, resulted georeferenced and digitized (Fig. 1a). The majority of the boreholes used in this study derive from different stratigraphic datasets held by INGV and related to previous geological investigations in the city of Rome, while an additional dataset of about 170 boreholes, executed and owned by Metro C S.p.A., (hereinafter MC) originates from the geognostic studies carried out during the preliminary works for the construction of Line C, section T3, of the Rome underground. (Romani et al., 2018).

The creation of the digital 3D model, in the third stage, was carried out by using the Leapfrog Works commercial software (Leapfrog Works, 2024) distributed by Seequent. Finally, stratigraphic correlations, guided by lithofacies and their lateral relationships, allowed the creation of a 3D geological model of a large portion of the historical center of Rome.

The final stage consisted of model validation. To validate the model, 4 new drillings (Fig. 2a) were performed within the Dynamic Planet ST-Predict project (Marra et al., 2024) and implemented in the GDB.

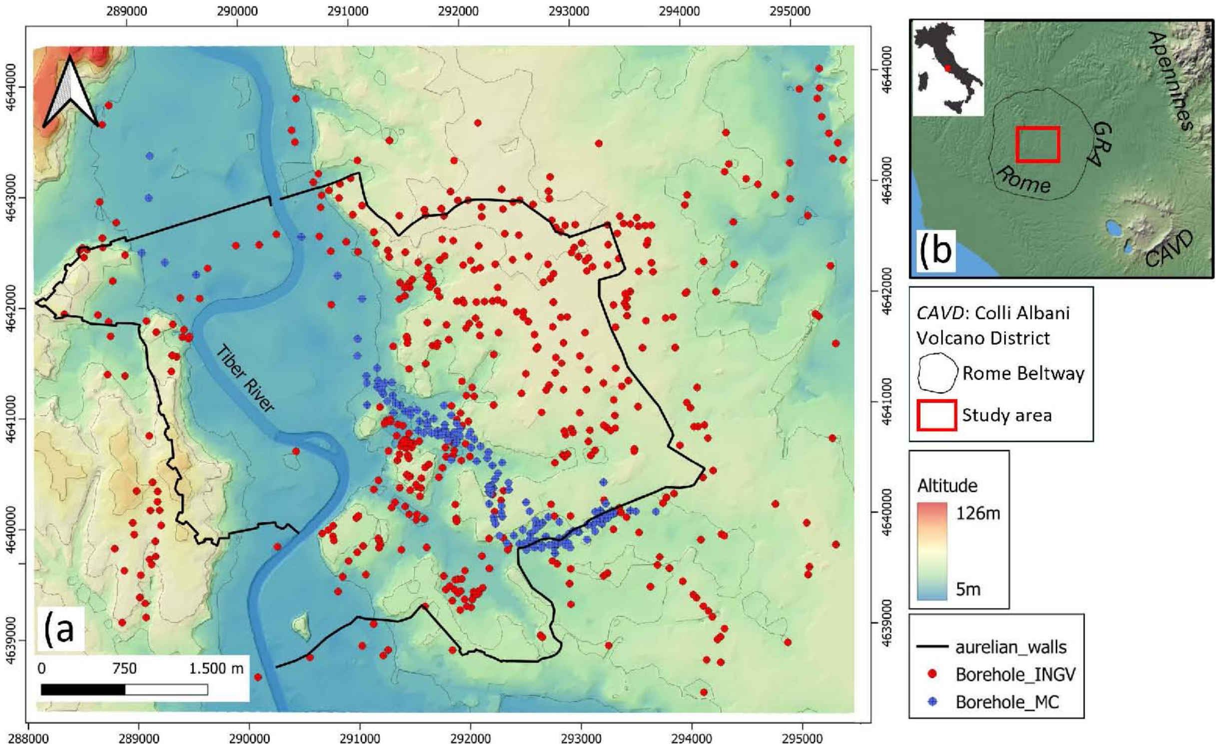

Figure 1. (a) Digital Elevation Model (DEM) of the study area. The map displays borehole locations from two different sources: blue dots represent boreholes from the Metro C archive, while red dots indicate boreholes from the INGV database; (b) Inset map showing the regional context of the Roman area, with the red box indicating the 3D modeling extent.

2. Geological setting

A complex stratigraphic setting characterizes the subsurface of Rome as a consequence of the interplay among different geodynamic factors which contributed to build up the geologic substrate (Funiciello et al., 2008a, 2008b; Luberti et al., 2017; Luberti and Monte, 2020; and ref. therein). A marine paleoenvironment characterized the Roman area since Messinian times throughout the Early Pleistocene, as a consequence of crustal extension due to the development of the Tyrrhenian back-arc basin (Parotto and Praturlon, 1975; Malinverno and Ryan, 1986). Since the Early Pleistocene, a regional uplift caused the progressive transition to continental sedimentation, carried out by a primitive drainage system of the Paleo-Tiber River (Marra and Florindo, 2014, and ref. therein). The oldest sediments outcropping in the city are represented by the Monte Vaticano Unit (MVU, Marra and Rosa, 1995; Marra et al., 1995; Cosentino et al., 2009), which consists of alternating clay and sand from an infralittoral environment dating back to the Pliocene-Early Pleistocene period (3.5-2.1 Ma) and serves as a geologic bedrock for the entire Rome area (Bozzano et al., 2000). It is followed by transgressive littoral to continental sands of the Monte Mario Unit (1.8-1.4 Ma), which testify the progressive upwelling of the marine basins (Marra et al., 1995; Cosentino et al., 2009). These marine terrains are exposed on the right bank of the Tiber River, at the foothills of the Monte Mario, Vaticano, and Gianicolo hills (see Fig. 2b). Transitional to continental deposits were initially emplaced in the Paleo-Tiber delta, located in correspondence of the present urban area, since 1.3 Ma (Florindo et al., 2024). Deposition of these sequences preceded the start of the major explosive activity of Monti Sabatini and Colli Albani volcanic districts (MSVD and CAVD in Fig. 1b), which took place since ~0.6 Ma (Karner et al., 2001a; Marra et al., 2020). During the whole Middle-Upper Pleistocene, the geological framework of the Roman area was shaped by the dynamic interaction between glacio-eustatic sea-level fluctuations, tectonic activity and volcanic eruptions. Erosion predominated during periods of falling sea levels, while sediment deposition occurred during periods of rising sea levels, filling in previously excavated channels ("Aggradational successions"; Marra et al., 2008, 2016a; Marino et al., 2025).

Each of the aggradational successions recognized in the Roman area is characterized by a basal, coarse gravel layer, abruptly transitioning upward to a thick package of sandy-clayey sediments, and it has been correlated with a phase of sea-level rise at the end of each of the glaciations that occurred in the last million years.

These successions are formally indicated with the number of the isotopic stage which follows the glacial termination (i.e. the highstand) and with a "Formation" name, generally inherited from that of the successions already recognized in the geological literature (Fig. 2a). Since the beginning of the major explosive volcanic activity around 0.6 Ma (Fornaseri et al., 1963; De Rita et al., 1995, 1995; Giordano et al., 2006; Gaeta et al., 2016; Marra et al., 2009, 2020), the sedimentary processes were significantly influenced by volcanic eruptions, which deposited large volumes of pyroclastic material, and by fault movements (Marra and Florindo, 2014; Luberti et al., 2017, and ref. therein).

Outcrops of the syn-volcanic sedimentary deposits occur alongside the current Tiber River valley and were deposited in recurring cycles corresponding to the post-glacial periods of sea-level rise, concurrently with the emplacement of the volcanic products. The Valle Giulia, S. Paolo, Aurelia and Vitinia Formations (Conato et al., 1980; Marra and Rosa, 1995; Karner and Marra, 1998) are continental formations referred to in literature as a syn-volcanic unit. They usually comprise fluvial and lacustrine deposits that contain reworked volcanic deposits.

A well-defined hydrographic network, with valleys characterized by prominent and steep banks that delimit the alluvial plains, shapes the Rome area because of the tectonic uplift of about 50 m that occurred in the last 250 ka (Karner et al., 2001b; Marra et al., 2016b). Deeply incised alluvial valleys are filled by unconsolidated, water-saturated sandy-clayey sediments (Corazza et al., 1999; Bozzano et al., 2008; Mancini et al., 2013; Marra et al., 2013).

The marked geomorphological characteristics, which at the end of the last glacial period gave rise to the tuffaceous cliffs that constitute the famous seven hills, are partially obliterated in the urban area, where over 2,000 years of anthropic activity have profoundly modified the original morphology, both through excavations, and with large thicknesses of fills to level out the depressions (Del Monte et al., 2016; Vergari et al., 2020).

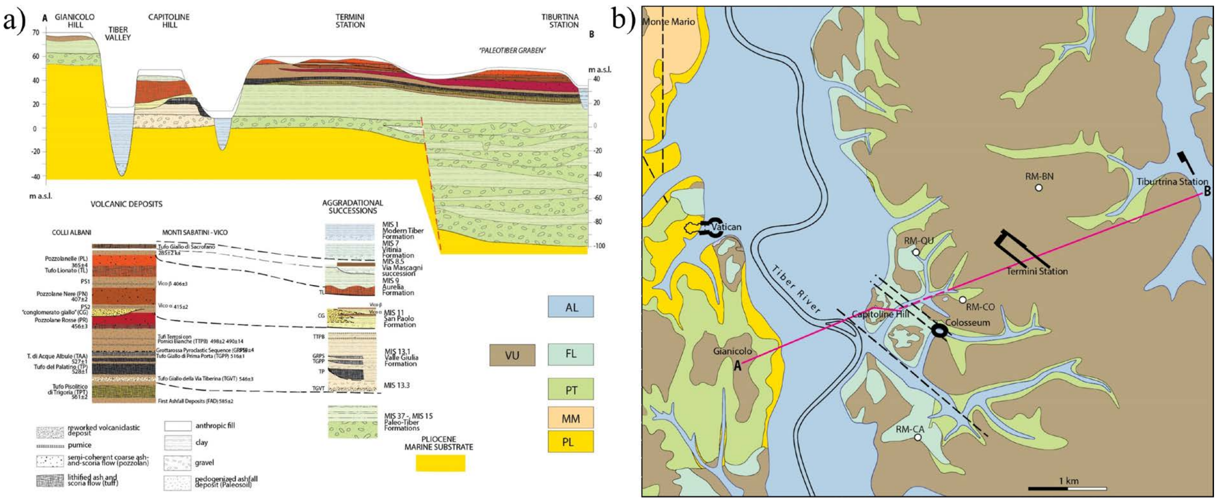

Figure 2. (a) Detailed stratigraphic scheme showing the geologic setting in the subsurface of Rome along the A-B cross-section (trace in the map, modified from Marra et al., 2024; ages in ky or referred to marine highstands); (b) simplified geologic map; the stratigraphic units are grouped into the six lithotypes used for the 3D modeling (refer to Table 1 for a detailed description of AL, VU, FL, PT, MM, PL).

3. GIS-based stratigraphic geodatabase

The core challenge in geological modeling is obtaining a robust 3D model from the analysis of 1D and 2D datasets, which constitute the primary sources of information. The accuracy of the resulting model strongly depends on high-quality borehole logs, and while the integration of geophysical data would further enhance reliability, in this study such data were not used, as the available cross-hole tests are confined to a limited sector of the study area. Given the stratigraphic complexity of the historical center of Rome, the model was therefore constructed exclusively based on stratigraphic information. As shown in Fig. 3, the methodology adopted in this work follows a systematic workflow to address these challenges and build a realistic 3D geological model.

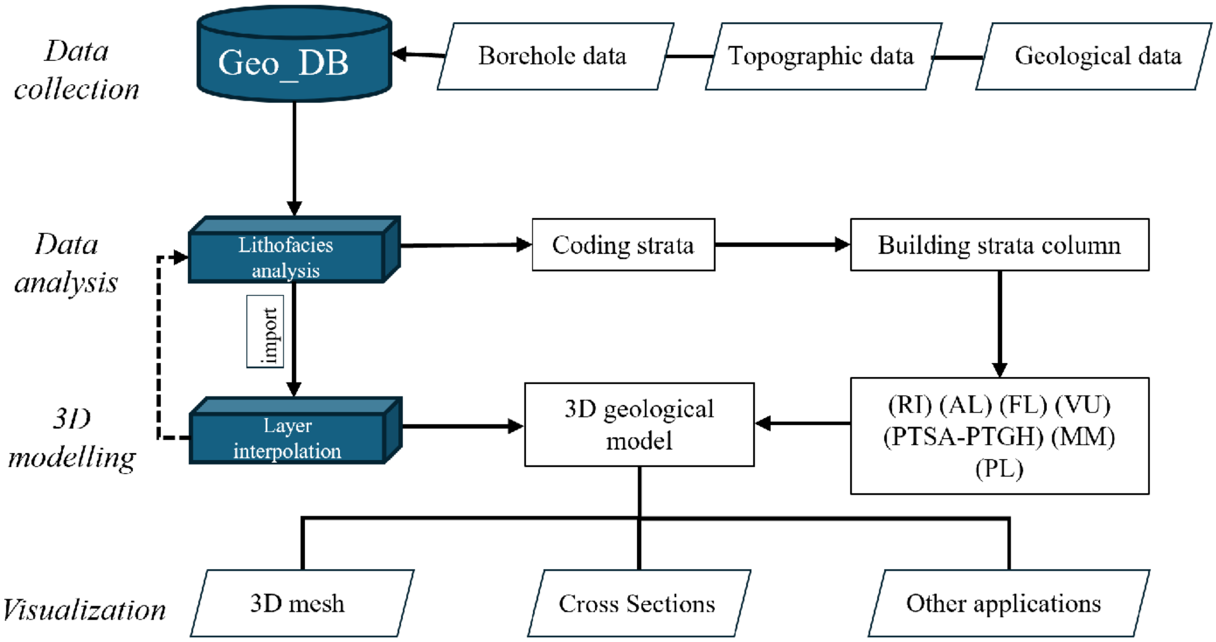

Figure 3. Flowchart illustrating the methodology for developing the 3D geological model.

3.1 Input Data

The process of building the GDB began by analysing the reports of ~800 stratigraphic continuous-core boreholes (Fig. 1a). These reports provide essential details about each borehole, including the well log and project descriptions, location (coordinates and elevation) and geometry (ex. drilling depth, dip, and azimuth) of the investigation. To identify representative lithofacies within diverse borehole data, each stratum was categorized using identification codes, specifying thickness and depth. A digital elevation model (DEM) was generated from surveyed points and contour lines extracted from the Regional Digital Technical Map, based on the classes of the Geotopographic Database of the Lazio Region (https://geoportale.regione.lazio.it), at 1:5,000 scale. The interpolation of elevation data produced a raster DEM with a cell size of 2 m. The spatial resolution of the DEM highlights the main morphological features of the area, represented by the Seven Hills (50-60 m a.s.l.) on the eastern bank of the Tiber River and the Monte Mario-Gianicolo ridge on the western bank, with an elevation of 139 m a.s.l. (Fig. 2b).

3.2 Standardization of borehole data

Conventionally, borehole data are described in a variety of formats tailored to different project requirements and organisational frameworks. Moreover, in densely urbanized areas, such as Rome, several infrastructure projects are currently underway, ranging from road construction to metro extensions and multi-storey buildings construction. Site investigations for these works are overseen by a wide range of geotechnical companies, including both public research institutions and private geotechnical laboratories. As a result, geotechnical reports from different projects can vary in format, data types, stylistic attributes and layout configurations. However, this vast and diverse range of geotechnical data relevant to Rome requires a standardised, structured and efficiently archived system. The borehole standard for the database must be meticulously tailored to integrate extensive and varied lithological data, mitigating data inconsistencies and redundancies, while accommodating the multifaceted nature inherent in geotechnical reports. Therefore, the presented method has been conceived with the main goal to implement the GDB by properly organising the management of lithostratigraphic data from various datasets collected over decades of subsurface investigations in the city of Rome (Marra et al., 2024).

3.3 Lithofacies coding

Lithofacies analysis stands out as a key element in a reliable reconstruction of subsurface stratigraphy and geological setting, providing a consistent representation of the sedimentary and tectonic configurations, and their geometric characteristics. In complex geological terrains, as exemplified by the investigation of the Roman subsurface, lithofacies analysis requires to merge fundamental geological knowledge with ancillary data, including stratigraphic contact types, which are essential for the construction of accurate 3D geological models. However, the description of stratigraphic logs is often subjective, and this may be misleading for 3D modeling purposes. Such limitations are particularly evident in the volcanic succession of the Rome area, which is constituted by a large number of eruption units characterized by different mechanisms of emplacement and lithologic-petrographic features, and for the products of their reworking, which are interlayered with the primary deposits and with the fluvial-lacustrine successions. Moreover, boreholes that are usually performed for civil engineering purposes are aimed at assessing the mechanical characteristics of the cored rocks (e.g., texture, grain size, deformability, shear resistance, etc.), independent from their correct chronostratigraphic attribution. Combined with the high degree of lateral variability, both within the same eruption unit, and taking into account the complex pattern of unconformity limits among the different units, such characteristics make any distinction based on the stratigraphic log description to be challenging.

Anthropogenic deposits (RI), as detailed in Table 1, constitute the uppermost stratigraphic units represented in the model. These deposits are consistently recognized and described across all analyzed stratigraphic logs, particularly within densely urbanized settings such as the old city of Rome. In order to ensure consistent data standardization, structural remains of anthropogenic artifacts from the Roman and Medieval periods encountered within the shallow subsurface, have been systematically classified as anthropogenic fill.

Holocene alluvial deposits (AL in Table 1) are characterized by a high degree of heterogeneity in their stratigraphic descriptions, and the identification of the basal contact with underlying units is often ambiguous due to variable lithological transitions and incomplete documentation. Where sufficiently detailed, these deposits exhibit granulometric and compositional features typical of fluvial environments, including sands, clays, organic-rich horizons, organic matter layers, and intercalated volcanic material. Spatially, they are confined within relict fluvial incisions that correspond to paleo-valleys of the former hydrographic network, such as the Velabrum, Murcia, and Labicano valleys (Marra and Rosa, 1995; Ammerman et al., 2000). These are now largely obscured by urban development. Deposit thicknesses show marked lateral variability, ranging from a few meters within narrow paleochannels—likely associated with ancient tributaries of the Tiber River—to thicknesses of approximately 60 m in the axial zone of the main alluvial basin, currently occupied by the modern Tiber River (see Appendix B).

The only reliable differentiation that has emerged from the analyses of stratigraphic logs concerns the lithified pyroclastic-flow deposits (tuffs), namely the Tufo del Palatino and Tufo Lionato, which present distinctive macroscopic aspects and mechanical characteristics (see Marra et al., 2024). However, even if these volcanic units have been identified and reported with a specific code in the geologic database, their discontinuous lateral extension and variable thickness make their 3D reconstruction based on rarefied point data poorly constrained. Consequently, all volcanic units have been grouped under a single code (VU in Table 1) for 3D modeling purposes.

Regarding the syn-volcanic fluvio-lacustrine successions (FL in Table 1), despite their seismic wave propagation behaviour similar to the analogous pre-volcanic units (Bozzano et al., 2008; Pagliaroli et al., 2013), they have been differentiated with a different code in the 3D model due to their more articulated spatial distribution compared to the tabular geometry characterizing the pre-volcanic deposits.

The sedimentary successions are characterized by fining-upward aggradational sequences, typically consisting of a basal coarse-gravel horizon, several meters thick, overlain by decametric layers of fine-grained sediments ranging from sand to clay.

In technical reports, the gravel horizons of the Paleo-Tiber succession (PT) are readily identifiable, whereas the finer-grained sediments are often poorly described. However, the lithological distinction between basal gravel horizons and the overlying sandy-clayey deposits is sufficient for reconstructing a 3D model aimed at defining local seismic response. Therefore, two different ID codes (PTGH and PTSA) have been attributed to gravel and sand deposits, respectively.

The Monte Mario Formation (MM in Table 1) outcrops in the right bank sectors of the Tiber River and it is represented by circalittoral deposits characterized by a basal silty-clayey unit that passes continuously upwards to grey and yellow sands.

The lowermost stratigraphic domain is represented by the Vatican Marls Formation, composed of overconsolidated Plio-Pleistocene clay (PL in Table 1). This domain constitutes the base of the 3D model and outcrops only in the western sectors of the Tiber valley. It is easily identifiable in borehole stratigraphic logs due to the sharp erosional contact with the overlying Paleo-Tiber gravel layer.

Table 1. Description of the lithofacies used in the geo-database and 3D modeling, showing their corresponding codes, age, and main sedimentological features such as color, texture, and composition. For simplification, certain lithofacies used here (e.g., AL, VU, FL) correspond to the merged units of the finer subdivisions proposed by Marra et al. (2024) (e.g., our AL combines their AL1 and AL2, and so on). In contrast, our PTSA and PTGH units correspond respectively to the PT1 and PT2 units in their original nomenclature.

Stratum code	Lithofacies	Main sedimentological features
RI	Anthropogenic deposits (Holocene)	Heterometric and heterogeneous elements within a predominantly pyroclastic sandy-silty matrix.
AL	Alluvial deposits (Upper Pleistocene-Holocene)	Sandy-silty and silty-clayey deposits variably interspersed with organic matter.
VU	Volcanic deposits (Middle Pleistocene)	semi-lithified to incoherent scoria-flow deposits (pozzolan), lapilli-sized to ash deposits, pedogenized ash deposit (paleosoil).
FL	Fluvial-lacustrine successions (syn-volcanic) (Middle Pleistocene)	Heterogeneous sedimentary complexes, consisting of sands, sandy silts, and variously intercalated clayey silts, with abundant volcanic minerals and lenses of reworked and altered pyroclastic materials.
PTSA	Fluvial-lacustrine deposits (pre-volcanic) (Middle-Lower Pleistocene)	Silty sands and sandy-clayey silts of yellow grey colour with calcareous concretions and local layers of travertine
PTGH		coarse gravel (ø ≤10 cm) in a sand matrix.
MM	Circalittoral deposits (Middle-Lower Pleistocene)	Clay and yellow sands with silty intercalations.
PL	Marine sediments (Pliocene – Early Pleistocene)	Overconsolidated clay, alternated with subordinate cm- to dm-thick yellow fine sand layers.

3.4 Geodatabase design and implementation

The focus in GDB design and implementation has been on how to store subsurface data and make it accessible not only for consultation but also to use these data dynamically for 3D processing and analysis. Therefore, the GDB has been implemented with inherited characteristics, so that starting from the surface location of the borehole data, all its other attributes have been expressed in terms of depth related to the ground surface. The investigation reports of the utilized boreholes provide details on (i) general information related to individual boreholes, including project specifications (borehole ID and survey year for MC boreholes), and (ii) specific details of the boreholes, such as location data (coordinates and elevation) and drilling depth details. Each record in the attribute table corresponds to a geological stratum, identified by a specific code (see Table 1), and contains information such as thickness and the absolute elevations of the top and bottom surfaces. The purpose of the GDB is to organize a large amount of data and to present lithological information in a clear, comprehensive, and effective manner.

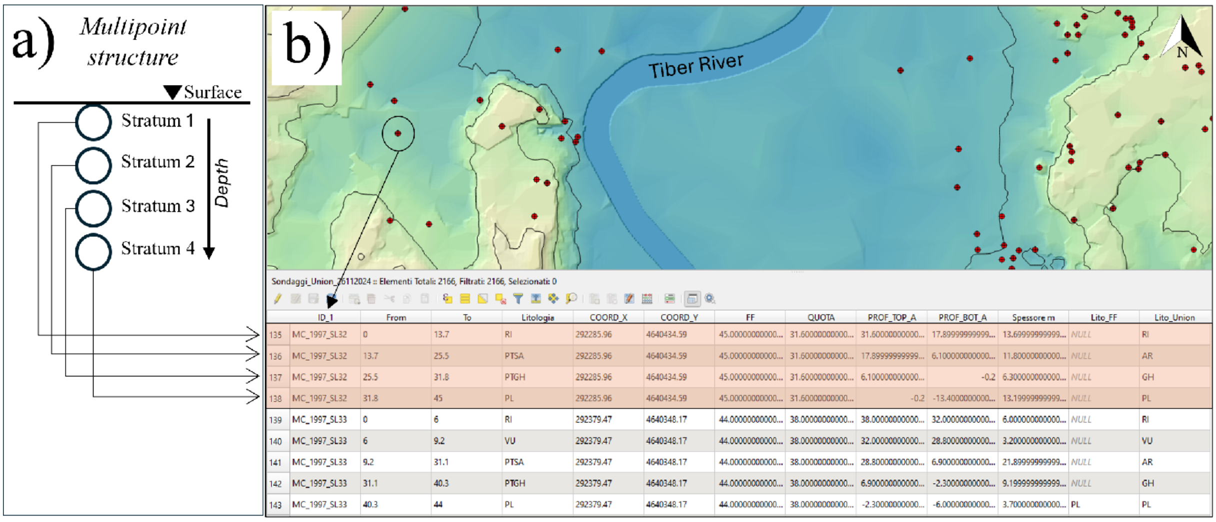

Figure 4. (a) Multipoint structure defined in the GIS based GDB; (b) Example of a borehole feature class (highlighted by a black circle) and its information in the related attribute table.

Database development was performed within the open-source QGIS software to visualize and analyse the 1D and 2D geological data in a spatial environment. The subsurface data structure essentially involves a relationship between a multipoint feature class, which allows for multiple points to be located in the same position (Fig. 4a) and an associated table containing the subsurface information (Fig. 4b). The created GDB contains various types of data, geometrically disaggregated, and organized into the following information layers, georeferenced and projected in the WGS84 UTM reference system, Zone 33N: (i) 2D linear topographic data, including contour lines, (ii) 1D multipoint data, including boreholes and spot elevation, and (iii) raster data, representing geological maps. Fig. 5 shows the 3D topographic surface of study area, illustrating elevation variations and morphological features, as generated from topographic data (contour lines, spot elevations and hydrography) available through the Lazio Region Cartographic Portal.

In the first version, the stratigraphy was represented with a high level of detail, distinguishing not only the main lithostratigraphic units but also, where identifiable, different volcanic units. This approach enabled a comprehensive stratigraphic description to be produced, which is useful for detailed geological analysis.

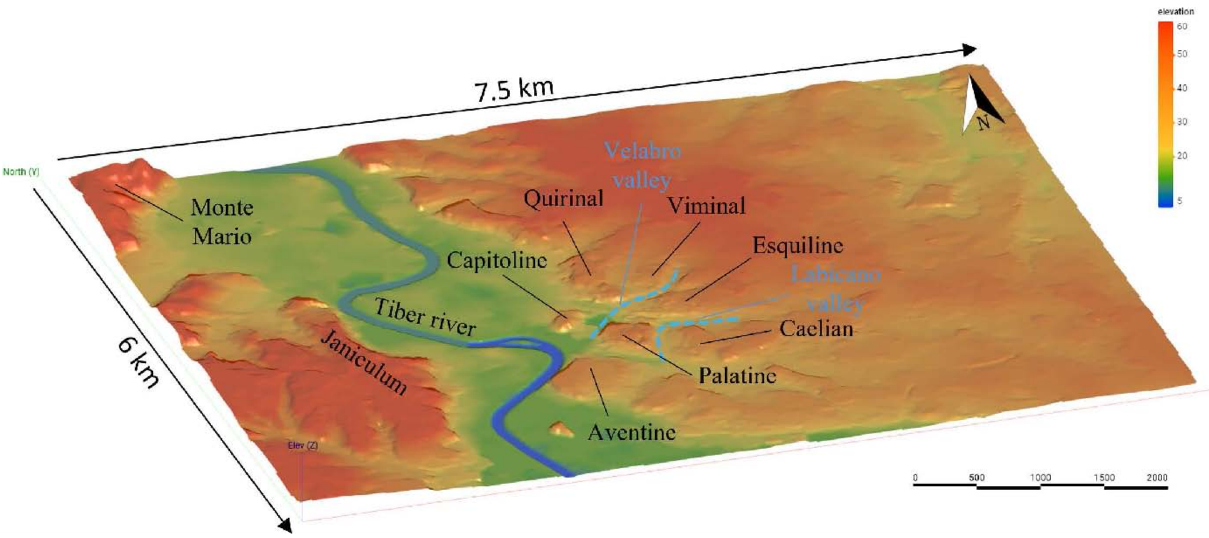

Figure 5. 3D topographic surface of study area with hill names, illustrating elevation variations and morphological features. The surface was generated from topographic data (contour lines, spot elevations and hydrography) available through the Lazio Region Cartographic Portal. Vertical (z) exaggeration is set to 2x to enhance terrain features recognition.

In the second version, the model was simplified by merging some units to reduce the complexity of the stratigraphic representation. This step improved data management and interpretation effectiveness while preserving a good descriptive capacity of the subsurface geological setting. Finally, in the third version here presented, the classification was further reorganized with a new nomenclature and a grouping criterion based on sediment characteristics. This adaptation responds to the specific needs of 3D modeling for seismic shear wave velocity estimation. In this context, the traditional stratigraphic subdivision was adjusted to prioritize the aggregation of lithological units based on their physical properties, enabling the delineation of geologically consistent domains for seismic velocity analysis. This evolution demonstrates how the structure of the geodatabase has been shaped by balancing stratigraphic accuracy with operational modeling requirements, with the structure adapting progressively to the specific emerging objectives of geophysical analysis. The GDB not only provides an effective representation of interpreted objects but also allows for efficient migration to various 3D modeling software's through export in different formats, such as tables in *.csv, *.txt formats.

4. 3D geological modeling

Over the decades, there has been a significant development and exploration of methodologies for modeling sedimentary systems in 3D. However, a crucial aspect of these techniques remains the definition and modelling of the top and bottom surfaces of each stratum (Zhu et al., 2012; Divya Priya et al., 2018). The explicit modeling process involves manually defining geological contacts and structures by digitizing 2D cross-sections, which are then linked to generate 3D bodies and surfaces. However, the manual approach to geological interpretation is time-consuming and prone to biases, resulting in unique and non-repeatable models (Cowan et al., 2003; Vollgger et al., 2015). In contrast, implicit geological modeling, introduced by Lajaunie et al. (1997), relies on data interpolation algorithms to define a continuous 3D function describing the spatial distribution of lithology (Rolo et al., 2017). Faults were not incorporated into the model because Leapfrog requires precise structural information (e.g., strike, dip, and geometry) that is not available in this case. In highly urbanized and anthropogenically modified areas, surface evidence of faulting is rarely preserved, and in addition, no seismic profiles extending to such depths are available to constrain their subsurface geometry.

Radial Basis Functions (RBFs hereafter) are versatile tools employed across various subsurface modeling applications. Commonly used for tasks like lithology interpolation (Cowan et al., 2003; Tan et al., 2014), RBFs can also be applied to construct 3D models of ore bodies from borehole data (Wang et al., 2018) and to predict mineral content in unconventional oil and gas reservoirs (Tan et al., 2012). RBFs interpolation offers a method to generate grid-free continuous functions valuable for representing geological structures (Martin and Boisvert, 2017; Vasuki et al., 2014). Isosurfaces extracted from these functions effectively represent geological structures, eliminating the need for manual digitization. Consequently, implicit modeling emerges as a time-efficient alternative to explicit methods, enabling quick updates with new drill hole data (Cowan et al., 2003; Boyle and Latscha, 2013).

4.1 Building 3D implicit lithological model

An implicit 3D geological model of the Quaternary deposits beneath the historic center of Rome was developed by integrating surface geology data with stratigraphic logs. Its construction was carried out using the Leapfrog Works geological modeling software (Seequent, 2024), which enables the interpolation of available geological information and provides a continuous and coherent representation of subsurface volumes. The 3D modeling was coded according to the scheme presented in Table 1, facilitating the categorization and management of stratigraphic information. This simplified approach ensures that surface interpolation respects the spatial distribution and continuity of lithofacies while preserving the geological integrity of the model, as shown by the A-B section in Fig. 7, which reflects the lithologic trend highlighted by the section in Fig. 2b (from Marra et al., 2024). Six representative geological cross-sections derived from the model are provided in Appendix A, and their traces are shown in Fig. 6. The 3D lithostratigraphic model was carried out considering only the main lithostratigraphic units identifiable in stratigraphic logs and distinguished by specific depositional characteristics. This method effectively delineates the spatial distribution and overall geometry of the primary geological domains while not accounting for internal heterogeneity and minor lithological transitions.

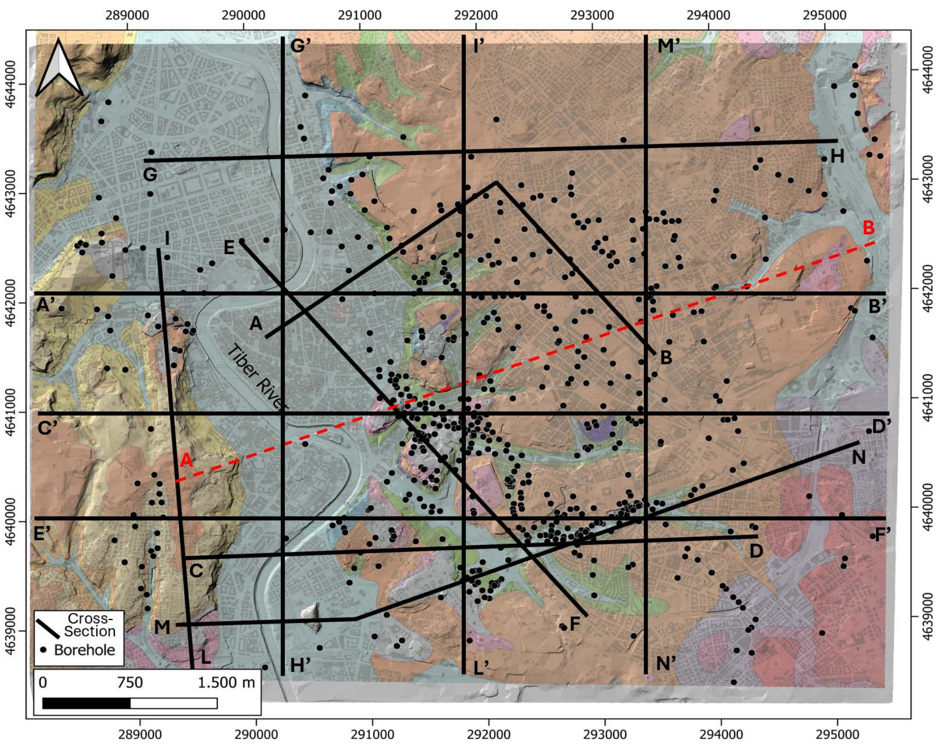

Figure 6. Map of the study area illustrating the traces of the six representative geological cross-sections presented in Appendix A, which provide additional insights into the subsurface architecture and complement the 3D lithostratigraphic model. The red dashed line corresponds to the trace of the cross-section shown in Fig. 2b.

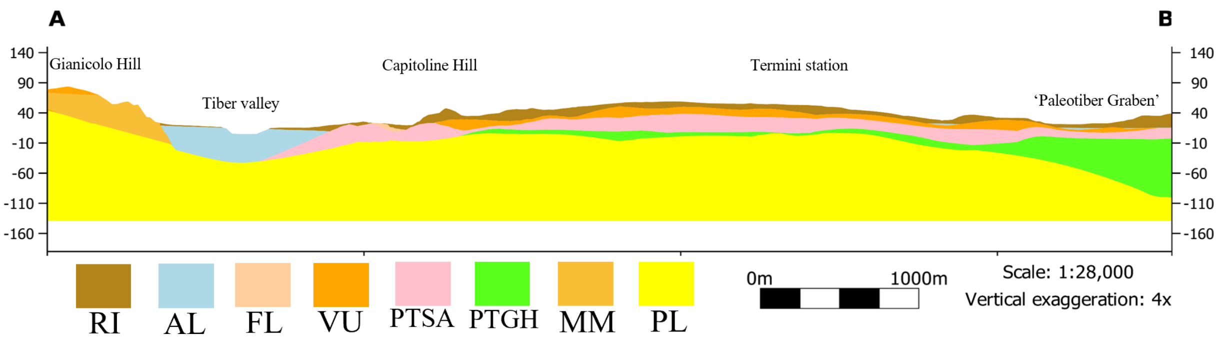

Figure 7. Geological cross-section generated in Leapfrog Geo, illustrating the lithologic architecture of the subsurface in the study area. The section trace, trending SW-NE, is shown in Fig. 2b and Fig. 6.

The 3D geological model covers an area of ca. 45 km^2 and extends to a depth of 160 m b.s.l. (Fig. 6). The reconstructed 3D domains can be described as follows (see Fig. 8):

- Anthropogenic deposits (RI) are present in all analyzed boreholes, continuously overlying all geological units across the entire study area. They have been reconstructed as a spatially continuous geological body, following the current topography with thicknesses ranging from a minimum of 0.5 m to a maximum exceeding 20 m (see Appendix B).
- The main alluvial deposits (AL) filling the extensive floodplain of the Tiber River are modelled with sufficient accuracy, unlike the narrow paleo-valleys with a NE-SW orientation (Labicano and Velabro streams, Fig. 5), which present greater modeling challenges.
- Volcanic deposits (VU) pose several challenges related to their reliable identification in borehole stratigraphic logs, mainly due to difficulties in precisely distinguishing different depositional mechanisms and their lithological and petrographic characteristics. For this reason, individual volcanic units were not classified separately; instead, the entire volcanic domain was represented as a single depositional body (Fig. 8). This domain predominates

within the study area, with the exception of the Tiber floodplain and the paleo-valleys that have been filled with recent alluvial deposits. However, the scarcity of stratigraphic boreholes in some parts of the model prevented from a complete volumetric reconstruction, resulting in some areas being left unmodeled.

- The syn-volcanic fluvio-lacustrine formation (FL) exhibits strong discontinuities, due to the complex geometry deriving from erosional and infill processes (Marra et al., 2024), which makes it difficult to interpretation challenging. Furthermore, these deposits have been influenced by eruptive activity and local tectonics, which made their stratigraphic setting complicate and so the reconstruction of successions and erosional contacts.
- The pre-volcanic Paleo-Tiber successions are easily recognizable based on their stratigraphic position, occurring between the overlying volcanic succession and the underlying Pliocene marine clay substrate. For the purpose of evaluating local seismic response, a lithostratigraphic distinction has been adopted between the basal gravel horizons (PTGH) and the overlying sandy-clayey horizons (PTSA). The Paleo-Tiber sedimentary body exhibits a tabular geometry and apparent lateral continuity, predominating in the eastern sector of the study area, where it is bounded to the west by the deep incision of the Tiber valley (see Appendix A). The 3D model of this unit reveals distinctive characteristics; for instance, the geometry of the gravel-dominated layer suggests higher shear-wave velocity (650-700 m/s) compared to the sandy-clayey part (400 m/s), attributable to its grain size composition and the degree of deposit compaction (Sbarra et al., 2012; Fäh et al., 1995; Rovelli et al., 1995).
- The Monte Mario Formation (MM) covers limited sectors of the structural highs west of the large Tiber River valley. This unit consists of circalittoral and littoral sands, representing the progressive uplift of the area.

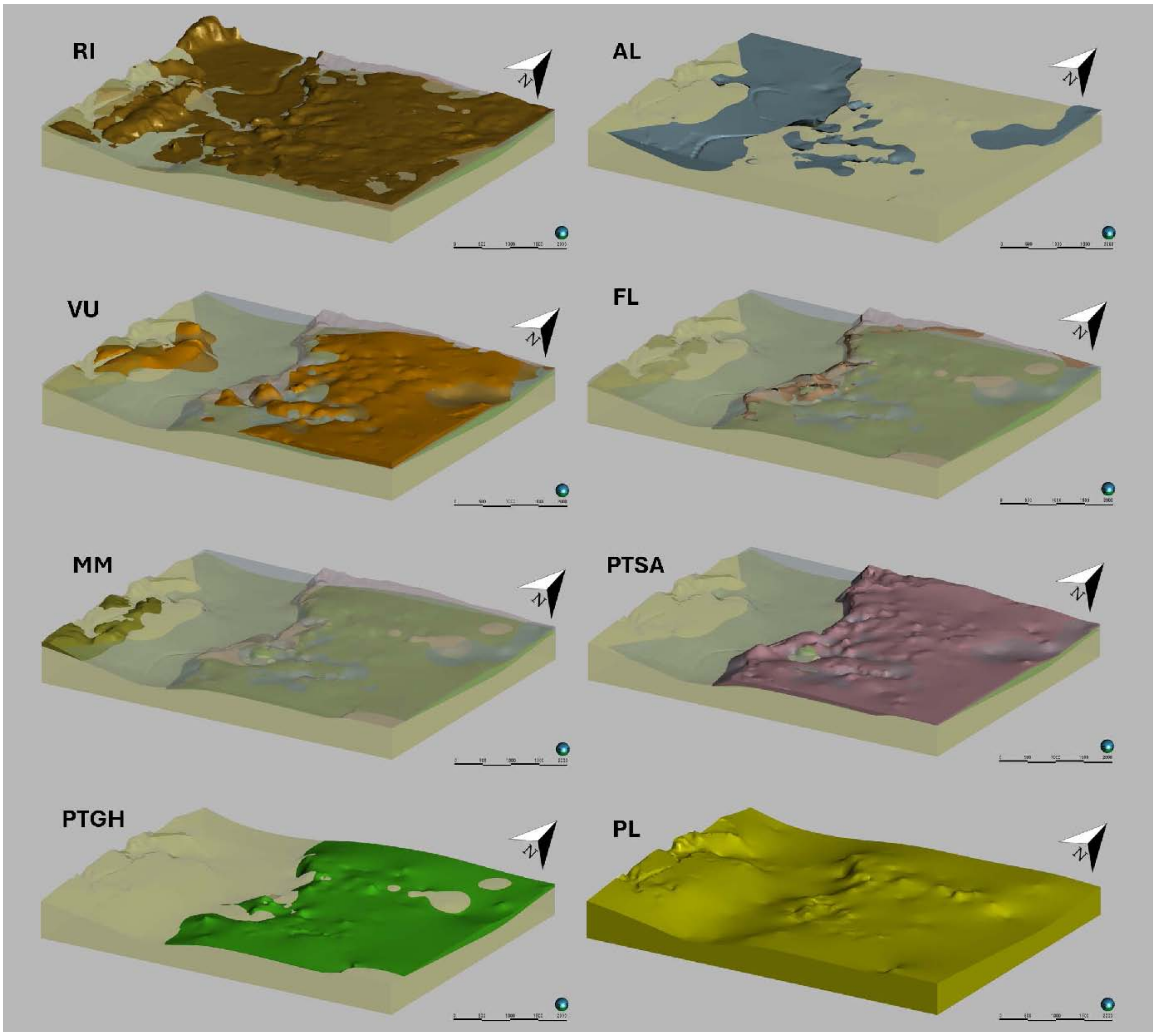

Figure 8. The 3D geological domains with their respective codes, modeled using Leapfrog Works software with RBF interpolation algorithms.

– The lowermost stratigraphic domain is represented by the Monte Vaticano Formation, composed of overconsolidated Plio-Pleistocene clay (PL). This 3D domain constitutes the base of the 3D model and, as already mentioned, crops out only in the western sectors of the Tiber valley. It is easily identifiable in borehole stratigraphic logs due to the sharp erosional contact with the overlying Paleo-Tiber gravelly layer.

4.2 Validation of the 3D model

The 3D geological model was validated through a rigorous comparative analysis, focused on assessing how much incorporating new stratigraphic data affects its accuracy and reliability. Two distinct models were constructed: one that excluded four boreholes drilled in 2024 and strategically located in key sectors of the study area to serve as control points for the model (Marra et al., 2024), and another one based on the complete set of available borehole data. The inset map in Fig. 9, panel a, shows the location of these boreholes. To evaluate their influence, acting as stratigraphic constraints, cross-sections that intersect the exact positions of these boreholes were generated. This allowed a direct comparison to be made between the interpolated geological surfaces of the two models (Fig. 9, panels b and c). Panel b shows the model incorporating the borehole data, while panel c shows the model without them.

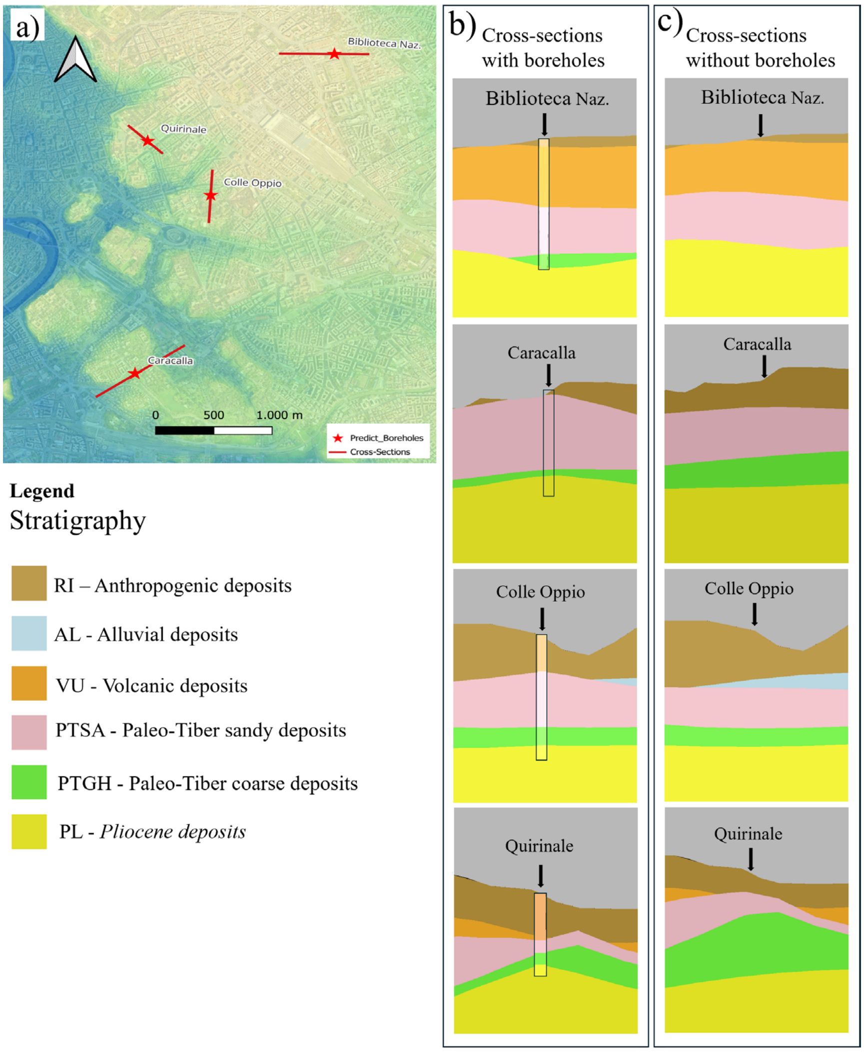

Figure 9. (a) Inset map illustrating the study area, including the location of additional 2024 boreholes carried out to refine the model and the traces of the 2D geological cross-sections (created using Leapfrog Works). (b) 2D cross-sections of the 3D geological model also incorporating stratigraphic data from the four 2024 boreholes. (c) Comparative 2D cross-sections of the 3D geological model without additional borehole data. Note the vertical exaggeration of 4x in the cross-sections.

This approach made it possible to quantitatively assess the changes in subsurface geometry and stratigraphic relationships resulting from the inclusion of the new drilling data. However, the trade-off between automation and user control becomes particularly evident when dealing with intricate geological features, where the software interpretation may diverge from expert geological knowledge. In some sectors of the study area, stratigraphy is especially complex and articulated; therefore, it is plausible that a geologist with specific expertise in the Roman stratigraphic framework might have proposed alternative reconstructions of the subsurface geometries. This interpretative variability reflects the intrinsic limitations of the implicit modeling approach adopted, which relies exclusively on borehole-derived constraints (x, y, z coordinates and the depths of lithological contacts). Such methodological constraints inherently reduce interpretative freedom and emphasize the preliminary nature of the model. Nevertheless, the resulting reconstruction provides geologically consistent and plausible stratigraphic geometries that align well with numerous previous studies on the subsurface of Rome, confirming the overall reliability of the modeling workflow. Despite the potential for customization in software such as Leapfrog Works (2024), the inherent limitations of automated interpolation may hinder accurate representation of complex subsurface structures, requiring substantial manual intervention to refine the model as shown in the Quirinale borehole (Fig. 9 panel c). In contrast, in sectors with a uniform data coverage, the automatic interpolation preserves the surface geometry and ensures that the thicknesses of lithostratigraphic units remain within geologically consistent and plausible ranges.

A notable advantage of the adopted methodology is the immediate updating of surfaces in response to the addition or removal of borehole data, providing a dynamic and responsive modeling environment. The ability to rapidly visualize the impact of new data on the geological model facilitates iterative refinement and enhances the understanding of subsurface geological conditions. In scenarios characterized by significant geological complexity and sparse data, the software works more effectively as a sophisticated 3D visualization tool rather than a precise volumetric model generator. Consequently, the primary utility lies in its ability to display and interact with geological data in 3D, enabling qualitative analysis and interpretation.

5. Discussion

The methodology described in this work allowed for an effective build-up of a 3D geological model, which provides a comprehensive representation of the subsurface geological setting of a study area. These models are essential tools, especially in geologically complex environments with significant lateral and vertical lithostratigraphic variability. A comprehensive geodatabase was created to manage drilling data and exported to Leapfrog for 3D modeling. The model simplifies the complex stratigraphy of Rome while defining the main lithostratigraphic units. It provides both a visualization of depositional architecture and a basis for future seismic simulations.

The lithofacies-based approach, while time-consuming, has proven particularly effective in reconstructing the subsurface setting of the Rome study area. Implicit 3D geological modeling software, while offering powerful tools for subsurface visualization and interpretation, encounters limitations when applied to complex geological scenarios, particularly those involving narrow incised valleys filled by alluvial sediments. These limitations often stem from the inherent mathematical algorithms and computational constraints employed by the software. While software packages can reproduce a range of conceptual geological models, respecting constraints given by well data – in this case study-, they may lead to challenges when dealing with intricate geometries and rapid spatial variations in lithology. The accurate representation of valley incisions is computationally intensive, requiring high-resolution meshes to capture their characteristic high aspect ratios and abrupt changes in slope. Furthermore, accurately representing the volume of these narrow valley fills is challenging for the software, mainly because the scarcity of borehole data in some areas introduces significant uncertainty in subsurface models (Fig. 10a and 10b). The inability to directly incorporate geological map data, such as U-shaped valley boundaries, as explicit constraints on the 3D surfaces presents another significant challenge. Often, the high level of detail contained within geological models is difficult to capture properly with inaccurate models. This necessitates a reliance on indirect methods, such as the manual digitization of valley margins and the subsequent imposition of these digitized polylines as constraints during the surface interpolation process. For this reason, despite its speed and utility, implicit modeling may not yet be fully mature for complex stratigraphies in urban environments.

The main limitations of the current model are associated with areas where the density of boreholes is lower, leading to discontinuous interpolations and less reliable geometries. Addressing this limitation in future

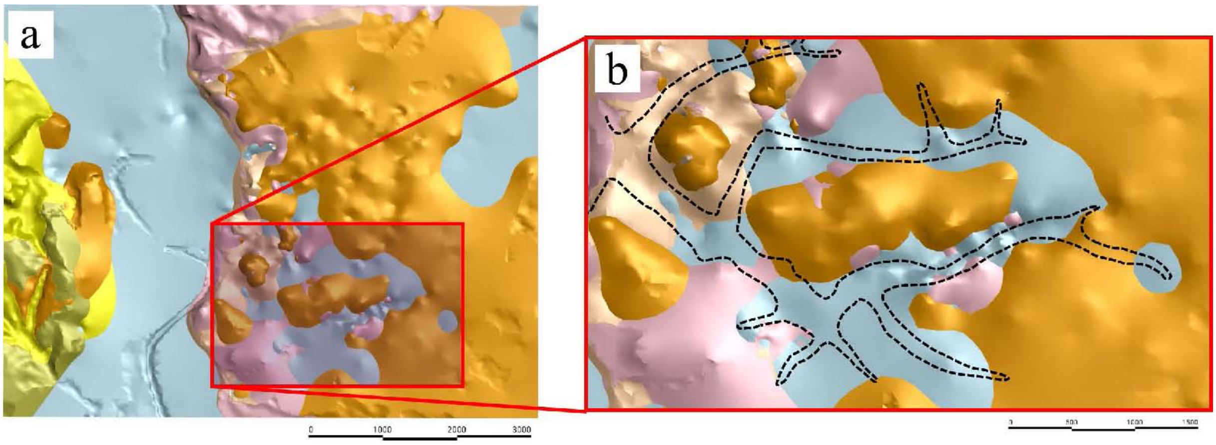

Figure 10. (a) Zenit view of the 3D geological model after removing the anthoropogenic fill. (b) Detail of the alluvial valley fill, highlighting the mismatch between the modeled alluvial deposits and the mapped geological boundaries (dashed black line), indicating a discontinuity in the modeled volume.

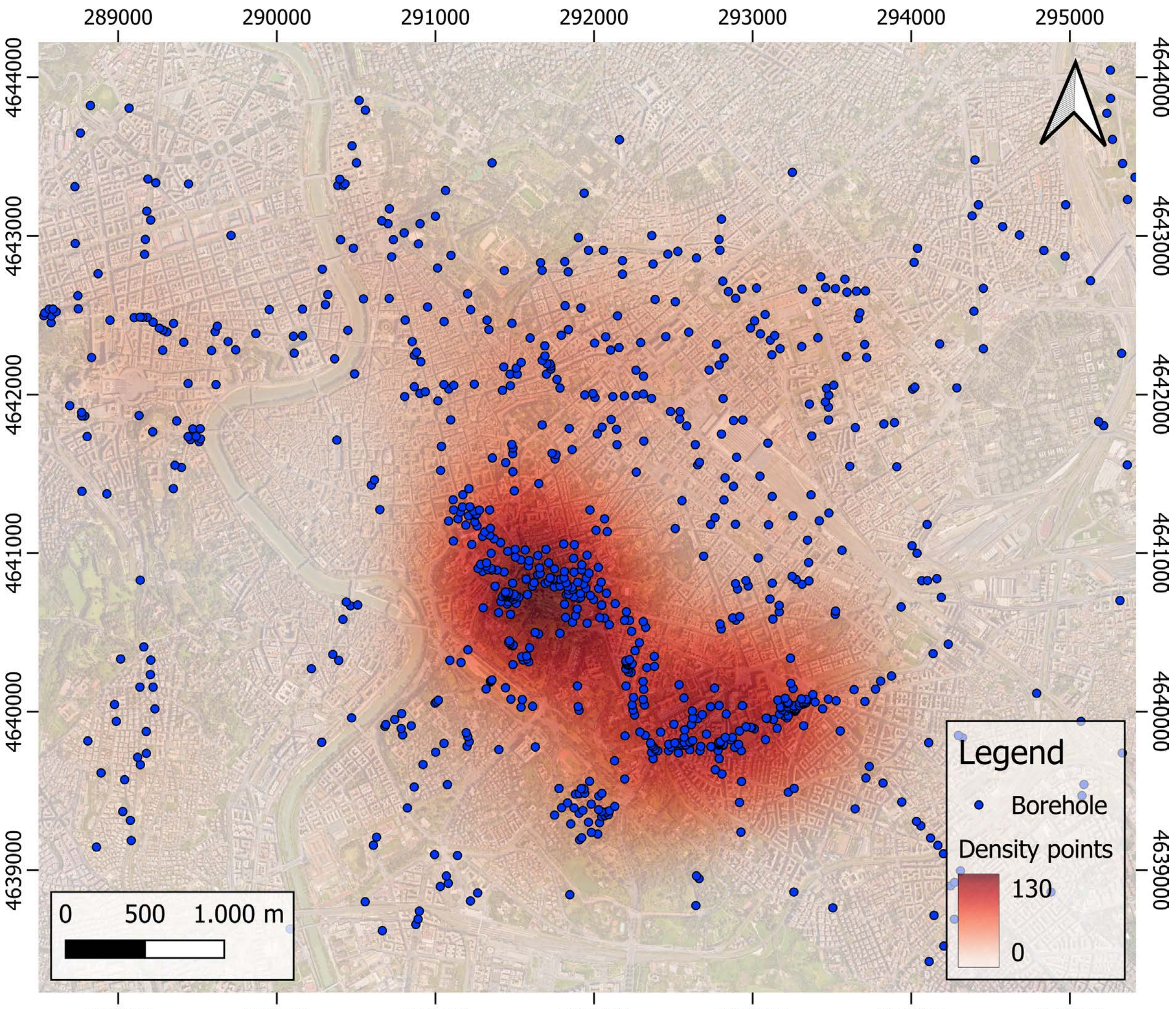

Figure 11. Map showing the spatial concentration of borehole survey points and corresponding local density. Blue circles indicate the location of the boreholes, while the red shading highlights areas of higher concentration, with density values ranging from 0 to 130 points per unit area.

developments requires the incorporation of additional subsurface information and the refinement of stratigraphic constraints. To this purpose, an indirect integrative workflow is currently being applied to improve the model in sectors characterized by limited borehole coverage. The method involves extracting 2D geological cross-sections from the existing explicit 3D model generated in Leapfrog. These sections are subsequently imported into ESRI™ ArcGIS Pro, where they are manually digitized and refined to include additional stratigraphic and geometrical detail derived from both the available surface and subsurface geological data. This integrative procedure enables a more robust representation of subsurface geometries in poorly constrained areas, enhancing both the internal consistency and geological reliability of the final 3D model.

Regarding uncertainty assessment, in this work the evaluation was primarily qualitative and based on the spatial distribution and density of available borehole data (as show in Fig. 11). The surfaces reconstructed by the modeling software are considered more reliable in zones with greater data density, where interpretations are better constrained. Conversely, uncertainty is recognized as increasing in areas with sparser data coverage, although it has not been quantitatively assessed due to the limitations of available methods and lack of supporting data. This pragmatic approach to uncertainty evaluation aligns with recommendations found in relevant literature dealing with data-driven 3D geological models based on borehole information (ISPRA, 2022; Wiegel et al., 2024; Hyer et al., 2024). Such works emphasize that, while more sophisticated quantitative uncertainty estimations exist, they often require extensive data and expertise not always feasible in applied urban geological modeling. Therefore, the reliance on borehole density mapping serves as a first-order proxy for model confidence and spatial uncertainty, transparently communicating model limitations to end users.

6. Conclusions

In this study, we developed a coherent methodological workflow for the analysis and 3D modeling of subsurface stratigraphy in an urban context. The approach begins with the creation of an integrated geodatabase within a GIS environment, which allows systematic, reproducible, and updatable management of large and heterogeneous borehole datasets. This geodatabase forms the foundation for the subsequent step, in which borehole stratigraphies are spatially visualized and interpreted in terms of lithofacies. This enables consistent correlation and comparison of subsurface units and provides a robust framework for handling incomplete or variable datasets. Finally, the methodology integrates the processed data and lithofacies interpretations to generate a 3D conceptual model of the subsurface stratigraphy of the historic center of Rome. The resulting model demonstrates the effectiveness of the workflow in producing coherent subsurface geometries and illustrates the applicability of the proposed methodological approach for future studies in similar complex urban environments. general, volume definition by a 3D modeling software relies on mathematical interpolators that spatially correlate stratigraphic data. While the adopted 3D modeling approach offers several advantages, it is essential to recognize its inherent limitations so that any integration or application of the model takes these constraints into account. Based on the results of this study, the following conclusions can be drawn:

1) Implicit modeling has proven to be an effective approach for reconstructing the urban subsurface in a geologically complex setting. Stratigraphic correlation driven by lithofacies provides a plausible representation of sedimentary bodies and their geometry.
2) The primary challenge of this approach is the identification of depositional facies tops and bottoms based solely on borehole log descriptions. The reinterpretation of borehole data is time consuming and requires specific sedimentological expertise.
3) The analysis enabled the definition of multiple 3D depositional domains, both volcanic and sedimentary, each characterized by distinct morphologies and depositional processes.
4) The quality and density of input data significantly influence interpolation results. It was observed that sparse or low-quality data can lead to less reliable predictions, particularly in areas with limited data coverage.
5) In the construction of the 3D model, the functionalities of the Leapfrog Works modeling software were tested. Although the software offers a high degree of customization for automatic interpolation, in complex depositional settings, the generation of surfaces often results in excessive irregularity, producing geologically implausible geometries. Conversely, in areas where data distribution is homogeneous and the stratigraphy is regular, the software performs optimally. Overall, we can conclude that Leapfrog Works serves as an excellent tool for 3D rendering rather than a robust engine for geological modeling.

Acknowledgements. This research was conducted within the PhD program in Environmental Geological and Polar Sciences and Technologies (XXXVIII cycle, academic year 2022-2025) at the University of Siena, focused on the theme: Reconstruction of the three-dimensional geological structure of the subsurface in urban environments. The PhD position was directly funded by the Istituto Nazionale di Geofisica e Vulcanologia (INGV), through the "Progetto 'Centro Italia (DL50)', Decreto-legge del 24/04/2017 n. 50."
The study also benefited from the scientific collaboration with INGV researchers involved in the grant "Progetto INGV Pianeta Dinamico (ST-PREDICT)" (CUP D53J19000170001), funded by the Italian Ministry MIUR (Legge 145/2018).
We thank the general contractor Metro C S.c.p.A. for providing the stratigraphic logs of the boreholes along the T3 section of Rome subway's Line C, and specifically acknowledge Ing. Eliano Romani and dott. Geol. Ivan Mammone for their essential support.

References

Ammerman, A. J., J. Miller and S. Ramsay (2000). The mid-Holocene environment of the Velabrum in Rome, Quad. Soc. Preist. Protostor. Reg. Friuli-Venezia Giulia, 8, 9-20.

Bonilla, F., F. Bozzano, C. Gelis, A. C. Giacomi. et al. (2011). Numerical modelling of shaking effects due to strong motions on the Tiber alluvial deposits in Rome (Italy), Proc. Effects Surf. Geol. Seism. Motion, Santa Barbara, CA, USA, 23-26 Aug., doi:10.48550/arXiv.1607.05068.

Boyle, C. and A-A. Latscha (2013). Implicit geological modelling of iron ore deposits, Proceedings Iron Ore, The Australasian Institute of Mining and Metallurgy: Melbourne, 57-66.

Bozzano, F., A. Andreucci, M. Gaeta et al. (2000). A geological model of the buried Tiber River valley beneath the historical centre of Rome, Bull. Eng. Geol. Environ., 59, 1-21, doi:10.1007/s100640000051.

Bozzano, F., A. Caserta, A. Govoni, F. Marra et al. (2008). Static and dynamic characterization of alluvial deposits in the Tiber River Valley: New data for assessing potential ground motion in the City of Rome, J. Geophys. Res. Solid Earth, 113, B1, doi:10.1029/2006JB004873.

Burrough, P. A., R. A. McDonnell and C. D. Lloyd (2015). Principles of Geographical Information Systems, Oxford University Press, Oxford, 352, ISBN 9780198742845.

Conato, V., D. Esu, A. Malatesta and F. Zarlenga (1980). New data on the Pleistocene of Rome, Quaternaria Roma, 22, 131-176.

Corazza, A., M. Lanzini, C. Rosa and R. Salucci (1999). Caratteri stratigrafici, idrogeologici e geotecnici delle alluvioni tiberine nel settore del centro storico di Roma, Il Quaternario, 12, 2, 215-235.

Cosentino, D., P. Cipollari, L. Di Bella, A. Esposito et al. (2009). Tectonics, sea-level changes and palaeoenvironments in the early Pleistocene of Rome (Italy), Quat. Res., 72, 1, 143-155, doi:10.1016/j.yqres.2009.03.003.

Cowan, E., R. Beatson, H. J. Ross, W. R. Fright et al. (2003). Practical Implicit Geological Modelling, 5th International Mining Geology Conference, Dominy (Ed.), The Australasian Institute of Mining and Metallurgy, Bendigo, Victoria, 1.

Cotar, A. and M. Brilly (2008). Use of Normalized Radial Basis Function in Hydrology, AIP Conf. Proc., 1076 ,1, 29-32, doi:10.1063/1.3046266.

De Rita, D., R. Funiciello and M. Parotto (1988). Carta geologica del complesso vulcanico dei Colli Albani ("Vulcano Laziale"), Consiglio Nazionale delle Ricerche – Progetto Finalizzato Geodinamica, Gruppo Nazionale per la Vulcanologia, in collaborazione con ENEL-AGIP e Dipartimento di Scienze della Terra, Università degli Studi di Roma "La Sapienza", SELCA, Firenze, 1 carta geologica a colori (scala 1:50.000).

De Rita, D., C. Faccenna, R. Funiciello and C. Rosa (1995). Stratigraphy and volcano-tectonics, the volcano of the Alban Hills, The Volcano of the Alban Hills, Trigila R., (Ed.), Tipografia SGS, Roma, 33-71.

Del Monte, M., M. D'Orefice, G. M. Luberti, R. Marini et al. (2016). Geomorphological classification of urban landscapes: the case study of Rome (Italy), J. Maps, 12, 1, doi:10.1080/17445647.2016.1187977.

Di Salvo, C., M. Mancini, G. P. Cavinato, M. Moscatelli et al. (2020). A 3D Geological Model as a Base for the Development of a Conceptual Groundwater Scheme in the Area of the Colosseum (Rome, Italy), Geosciences, 10, 7, 266, doi:10.3390/geosciences10070266.

Di Salvo, C., M. Mancini, M. Moscatelli, M. Simionato et al. (2021). From Lithological Modelling to Groundwater Modelling: A Case Study in the Tiber River Alluvial Valley, Geosciences, 11, 12, 507, doi:10.3390/geosciences 11120507.

Divya Priya, B. and G. R. Dodagoudar (2018). An integrated geotechnical database and GIS for 3D subsurface modelling: Application to Chennai City, India, Appl. Geomat., 10, 2, 47-64, doi:10.1007/s12518-018-0202-x.

Fäh, D., C. Iodice, P. Suhadolc and G. F. Panza (1995). Application of numerical simulations for a tentative seismic microzonation of the city of Rome, Ann. Geophys., 38, 5-6, doi:10.4401/ag-4079.

Florindo, F., F. Marra, B. R. Jicha, F. Bulian et al. (2024). Glacier melting triggers massive gravel deposition in central Italy's river basins, unveiling deglacial events From 1250 to 780 ka, J. Geophys. Res. Solid Earth, doi:10.1029/2023JB027877.

Ford, J. R., S. J. Mathers, K. R. Royse, D. T. Aldiss et al. (2010). Geological 3D modelling: scientific discovery and enhanced understanding of the subsurface, with examples from the UK, Z. Dtsch. Ges. Geowiss., 161, 2, 205-218, doi:10.1127/1860-1804/2010/0161-0205.

Fornaseri, M., A. Scherillo and U. Ventriglia (1963). La regione vulcanica dei Colli Albani: Vulcano Laziale, Consiglio Nazionale delle Ricerche, Roma, XI, 561, OCLC: 1040869174.

Funiciello, R. and G. Giordano (2008a). Foglio 374 Roma, Note illustrative, Carta Geologica d'Italia, scala 1:50000, Dipartimento Difesa del Suolo, Servizio Geologico d'Italia, Roma, 158.

Funiciello, R. and G. Giordano (2008b). La nuova carta geologica di Roma: litostratigrafia e organizzazione stratigrafica, La geologia di Roma dal centro storico alla periferia, Mem. Descr. Carta Geol. Ital., 80, 39-85.

Gaeta, M., C. Freda, F. Marra, I. Arienzo et al. (2016). Palaeozoic metasomatism at the origin of Mediterranean ultrapotassic magmas: constraints from time-dependent geochemistry of Colli Albani volcanic products (Central Italy), Lithos, 244, 1, 151-164, doi:10.1016/j.lithos.2015.11.034.

Giacomelli, S., A. Zuccarini, A. Amorosi, L. Bruno et al. (2023). 3D geological modelling of the Bologna urban area (Italy), Eng. Geol., 324, 107242, doi:10.1016/j.enggeo.2023.107242.

Giordano, G., A. A. De Benedetti, A. Diana and G. Diano (2006). The Colli Albani mafic caldera (Roma, Italy): stratigraphy, structure and petrology, J. Volcanol. Geotherm. Res., 155, 1-2, 49-80, doi:10.1016/j.jvolgeores.2006.02.009.

Hyer, A. S., P. B. E. Sandersen, L. T. Andersen et al. (2024). Evaluating the chain of uncertainties in the 3D geological modelling workflow, Eng. Geol., 343, 107792, doi:10.1016/j.enggeo.2024.107792.

ISPRA (2022). Linee guida per la geologia di subsuperficie 3D, Istituto Superiore per la Protezione e la Ricerca Ambientale, https://www.isprambiente.gov.it.

Karner, D. B. and F. Marra (1998). Correlation of fluviodeltaic aggradational sections with glacial climate history: a revision of the classical Pleistocene stratigraphy of Rome, Geol. Soc. Am. Bull., 110, 6, 748-758, doi:10.1130/0016-7606(1998)110<0748:COFASW>2.3.CO;2.

Karner, D. B., F. Marra, F. Florindo and E. Boschi (2001b). Pulsed uplift estimated from terrace elevations in the coast of Rome: evidence for a new phase of volcanic activity?, Earth Planet. Sci. Lett., 188, 1-2, 135-148, doi:10.1016/S0012-821X(01)00325-9.

Karner, D. B., F. Marra and P. Renne (2001a). The history of the Monti Sabatini and Alban Hills volcanoes: groundwork for assessing volcanic-tectonic hazards for Rome, J. Volcanol. Geotherm. Res., 107, 185-219, doi:10.1016/S0377-0273(00)00258-4.

Lajaunie, C., G. Courrioux and L. Manuel (1997). Foliation fields and 3D cartography in geology: Principles of a method based on potential interpolation, Math. Geol., 29, 571-584, doi:10.1007/BF02775087.

Luberti, G. M., F. Marra and F. Florindo (2017). A review of the stratigraphy of Rome (Italy) according to geochronologically and paleomagnetically constrained aggradational successions, glacio-eustatic forcing and volcano-tectonic processes, Quat. Int., 438, 8, 40-67, doi:10.1016/j.quaint.2017.01.044.

Luberti, G. M. and M. D. Monte (2020). Landscapes and landforms connected with anthropogenic processes over three millennia: The Servian Walls at the Esquiline Hill (Rome, Italy), Holocene, 30, 12, 1817, doi:10.1177/0959683620950460.

Malinverno, A. and W. B. F. Ryan (1986). Extension in the Tyrrhenian Sea and shortening in the Apennines as results of arc migration driven by sinking of the lithosphere, Tectonics, 5, 2, 227-245, doi:10.1029/TC005i002p00227.

Mancini, M., M. Moscatelli, F. Stigliano, G. P. Cavinato, (2013). The Upper Pleistocene-Holocene fluvial deposits of the Tiber River in Rome (Italy): lithofacies, geometries, stacking pattern and chronology, J. Mediterr. Earth Sci., 5, 2, 95-101, doi:10.1029/TC005i002p00227.

Maojin, T., Z. Youlong and Guoyue (2012). Mineral content prediction for unconventional oil and gas reservoirs based on logging data, AIP Conference Proceedings, American Institute of Physics, Melville, NY, 1479, 1, 1923-1929.

Marino, G., F. Marra, B. Jicha, F. Bulian et al. (2025). The timing of the Middle Pleistocene Terminations based on 40Ar/39Ar Detrital Sanidine Dating, Paleoceanogr. Paleoclimatol., doi:10.1029/2024PA005050.

Marra, F. and C. Rosa (1995). Stratigrafia e assetto geologico dell'area romana, La geologia di Roma: il centro storico, Funiciello, R. (Ed.), Mem. Descr. Carta Geol. Ital., 50, 49-118.

Marra, F., M. G. Carboni, L. Di Bella, C. Faccenna et al. (1995). Il substrato plio-pleistocenico nell'Area Romana, Boll. Soc. Geol. Ital., 114, 195-214.

Marra, F., F. Florindo and E. Boschi (2008). History of glacial terminations from the Tiber River, Rome: insights to glacial forcing mechanisms, Paleoceanography, 23, 2, PA2205, doi:10.1029/2007PA001543.

Marra, F., D. B. Karner, C. Freda, M. Gaeta et al. (2009). Large mafic eruptions at Alban Hills Volcanic District (Central Italy): Chronostratigraphy, petrography and eruptive behavior, J. Volcanol. Geotherm. Res., 179, 217-232, doi:10.1016/j.jvolgeores.2008.11.009.

Marra, F., F. Bozzano and F. R. Cinti (2013). Chronostratigraphic and lithologic features of the Tiber River sediments (Rome, Italy): implications on the post-glacial sea-level rise and Holocene climate, Glob. Planet. Change, 107, 157-176, doi:10.1016/j.gloplacha.2013.05.002.

Marra, F. and F. Florindo (2014). The subsurface geology of Rome: Sedimentary processes, sea-level changes and astronomical forcing, Earth-Sci. Rev., 136, 1-20, doi:10.1016/j.earscirev.2014.05.001.

Marra, F., E. J. Rohling, F. Florindo, B. Jicha et al. (2016a). Independent 40Ar/39Ar and 14C age constraints on the last five glacial terminations from the aggradational successions of the Tiber River, Rome (Italy), Earth Planet Sci. Lett., 449, 105-117, doi:10.1016/j.epsl.2016.05.037.

Marra, F., F. Florindo, M. Anzidei and V. Sepe (2016b). Paleo-surfaces of glacio-eustatically forced aggradational successions in the coastal area of Rome: assessing interplay between tectonics and sea-level during the last ten interglacials, Quatern. Sci. Rev, 148, 85-100, doi:10.1016/j.quascirev.2016.07.003.

Marra, F., C. Castellano, L. Cucci, F. Florindo et al. (2020). Monti Sabatini and Colli Albani: the dormant twin volcanoes at the gates of Rome, Sci. Rep., 10, 1, 8666, doi:10.1038/s41598-020-65394-2.

Marra, F., C. Rosa, D. Silvestri, P. Bordoni et al. (2024). Predict: Assessing the Seismic Response in the city of Rome, Part 1. New Data for a Geologic Overview, Ann. Geophys., 67, 3, SE325, doi:10.4401/ag-9116.

Martino, S., L. Lenti, C. Gélis, A. C. Giacomi et al. (2015). Influence of Lateral Heterogeneities on Strong-Motion Shear Strains: Simulations in the Historical Center of Rome (Italy), Bull. Seismol. Soc. Am., 105, 5, 2604, doi:10.1785/0120140180.

Pagliaroli, A., G. Lanzo, P. Tommasi and V. Di Fiore. (2013). Dynamic characterization of soils and soft rocks of the Central Archeological Area of Rome, Bull. Earthq. Eng., 12, 1365-1381, doi:10.1007/s10518-013-9452-5.

Parotto, M. and A. Praturlon (1975). Geological summary of the central Apennines, structural model of Italy: Maps and explanatory notes, Quad. Ric. Sci., 1, 90, 257-311.

Regione Lazio (2022). Regional Technical Map 1:5000, Open Data Portal, accessed February 2022, https://dati.lazio.it/.

Romani, E., I. Mammone, S. Moretti and G. Pezzetti (2018). Rome Metro Line Monitoring System: The C Line experience, Proceedings of the International Symposium on Field Measurements in Geomechanics, PUC Rio, Rio de Janeiro, Brazil.

Rovelli, A., L. Malagnini, A. Caserta and F. Marra (1995). Using 1-D and 2-D modelling of ground motion for seismic zonation criteria: results for the city of Rome, Ann. Geophys., 38, 5, 591-605, doi:10.4401/ag-4075.

Ryan, M. and J. B. Boisvert (2017). Iterative refinement of implicit boundary models for improved geological feature reproduction, Comput. Geosci., 109, C, 1-15, doi:10.1016/j.cageo.2017.07.003.

Sbarra, P., V. De Rubeis, E. Di Luzio et al. (2012). Macroseismic effects highlight site response in Rome and its geological signature, Nat. Hazards, 62, 425-443, doi:10.1007/s11069-012-0085-9.

Seequent (2024). Leapfrog Works User Guide version 2.0. Seequent Limited, Christchurch, New Zealand, https://www.seequent.com/help-support/leapfrog-works/.

Stucchi, M., C. Meletti, V. Montaldo, H. Crowley et al.(2011). Seismic Hazard Assessment (2003-2009) for the Italian Building Code, Bull. Seismol. Soc. Am., 101, 1885-1911, doi:10.1785/0120100130.

Terrington, R., B. Napier, A. Howard, J. Ford et al. (2008). Why 3D? The Need for Solution Based Modeling in a National Geoscience Organization, AIP Conference Proceedings, American Institute of Physics, Melville, NY, 1099, 1, doi:10.1063/1.2937278.

Vasuki, Y., E.-J. Holden, P. Kovesi and S. Micklethwaite (2014). Semi-automatic mapping of geological Structures using UAV-based photogrammetric data: An image analysis approach, Comput. Geosci., 69, 22-32, doi:10.1016/j.cageo.2014.04.012.

Ventriglia, U. (1971). La Geologia della città di Roma, Amministrazione Provinciale di Roma, Roma, 417.

Vergari, F., G. M. Luberti, A. Pica and M. Del Monte (2020). Geomorphology of the historic centre of the Urbs (Rome, Italy), J. Maps, 17, 4, 6-17, doi:10.1080/17445647.2020.1761465.

Von der Tann, L., R. Sterling, Y. Zhou and N. Metje (2019). Systems approach to urban underground space planning and management-review, Underground Space, 5, 2, 144-166, doi:10.1016/j.undsp.2019.03.003.

Wang, J., H. Zhao, L. Bi and L. Wang (2018). Implicit 3D Modeling of Ore Body from Geological Boreholes Data Using Hermite Radial Basis Functions, Minerals, 8, 10, 443, doi:10.3390/min8100443.

Wiegel, A., A. Peña-Olarte and R. Cudmani (2024). Quantification and validation of uncertainties in subsoil models, Case study at the New Town Hall, Munich, Geotechnik, 47, 4, 269-281, doi:10.1002/gete.202400011.

Wu, J., J. Chen, G. Chen, Z. Wu et al. (2021). Development of Data Integration and Sharing for Geotechnical Engineering Information Modeling Based on IFC, Adv. Civ. Eng., ID8884864, doi:10.1155/2021/8884864.

Yu, L., D. Zhang, B. Xie and H. Zhang (2008). A new approach for subsurface space mapping of urban area using RS and GIS, Proc. SPIE 7144, Geoinformatics and Joint Conference on GIS and Built Environment: The Built Environment and Its Dynamics, SPIE, Bellingham, WA, 71441T, 5 November, doi:10.1117/12.812784.

Zhang, T. F. and K. Xiao (2013). Application of three-dimensional modelling in the study of complex geological body, Adv. Mater. Res., 709, 567-570, doi:10.4028/www.scientific.net/amr.709.567.

Zhang, T., P. Tilke, E. Dupont, L. Zhu et al. (2019). Generating geologically realistic 3D reservoir facies models using deep learning of sedimentary architecture with generative adversarial networks, 16, 541-549, doi:10.1007/s12182-019-0328-4.

Appendix A. Representative geological cross-sections

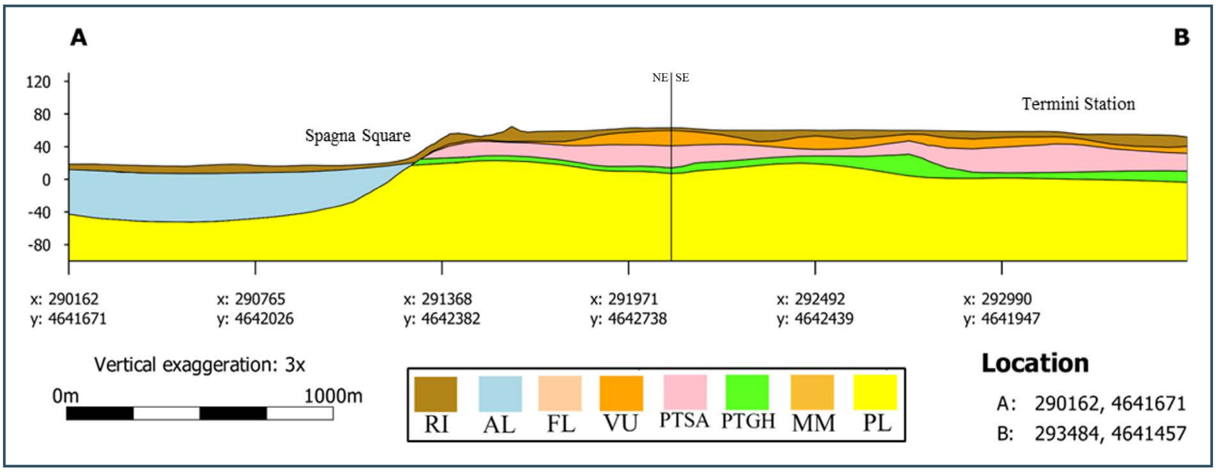

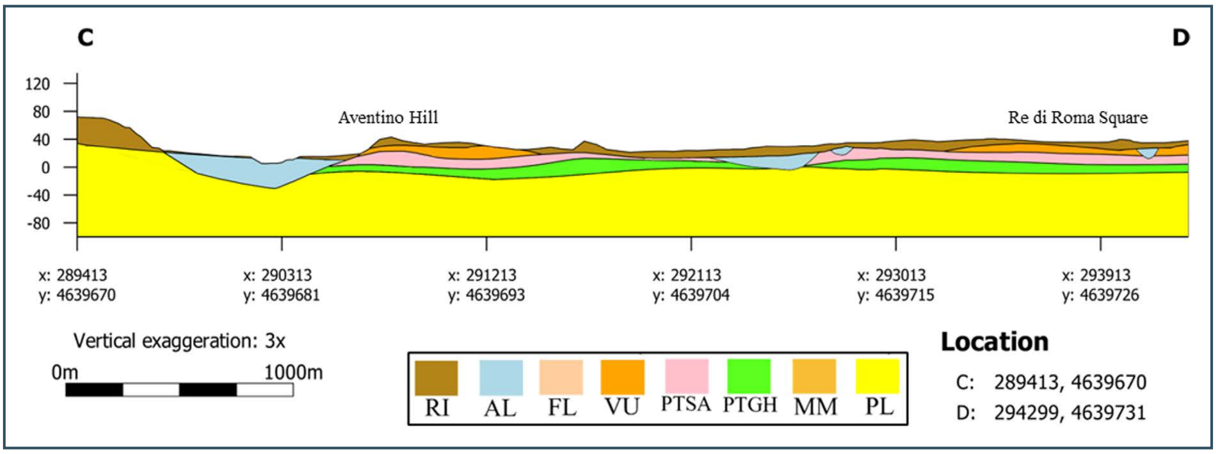

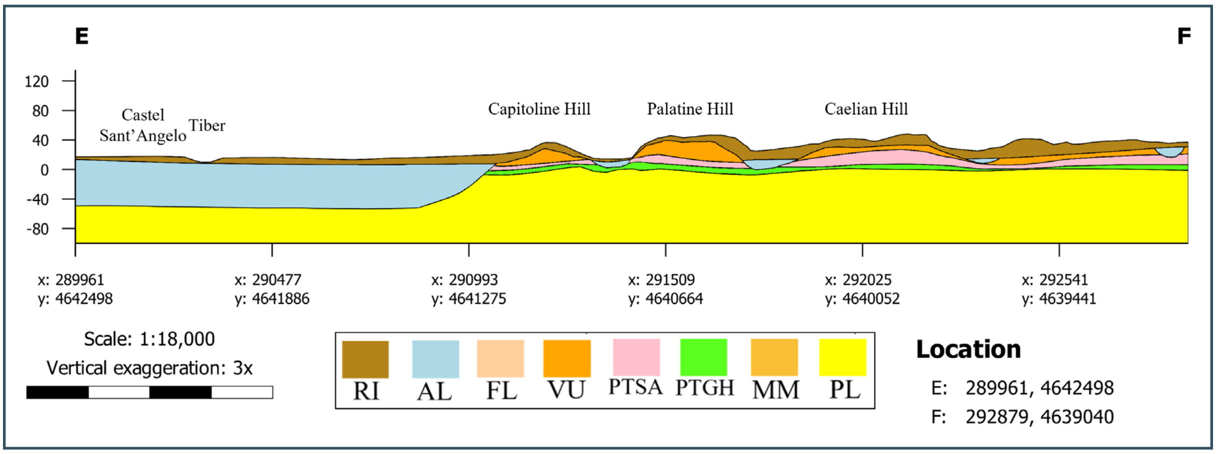

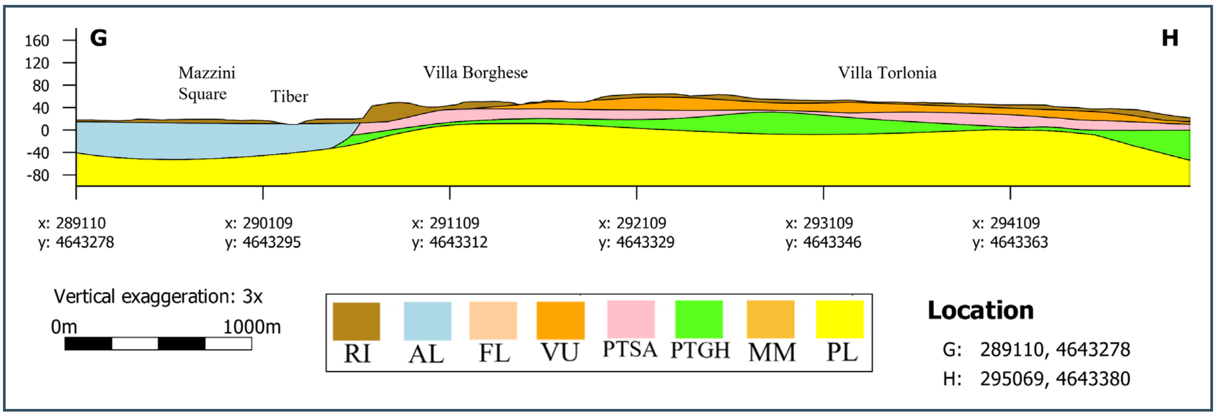

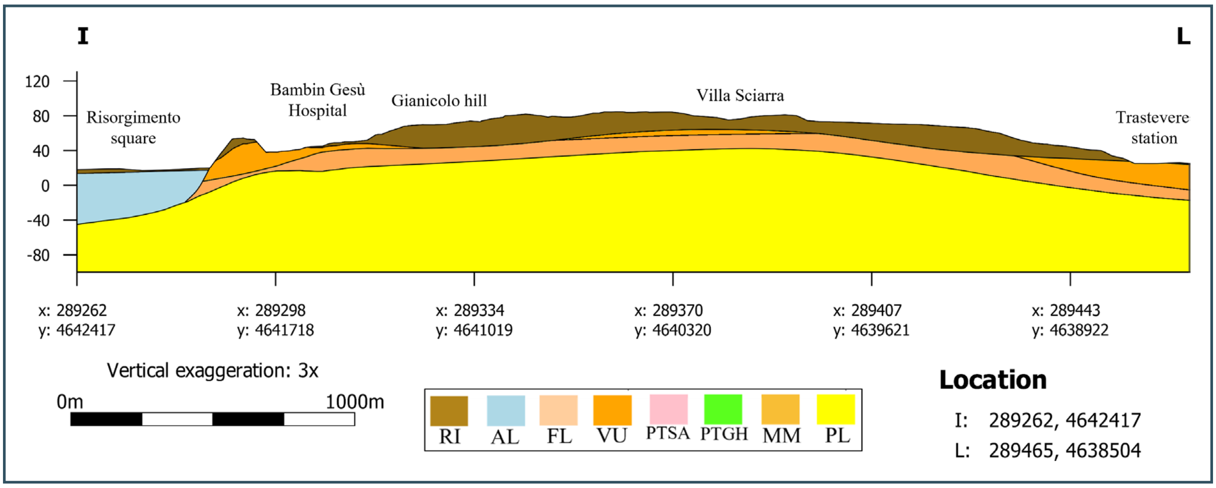
I
L
120
80
40
0
-40
-80
Risorgimento square
Bambin Gesù Hospital
Gianicolo hill
Villa Sciarra
Trastevere station
x: 289262 y: 4642417
x: 289298 y: 4641718
x: 289334 y: 4641019
x: 289370 y: 4640320
x: 289407 y: 4639621
x: 289443 y: 4638922
Vertical exaggeration: 3x
0m
1000m
RI AL FL VU PTSA PTGH MM PL
Location
I: 289262, 4642417
L: 289465, 4638504

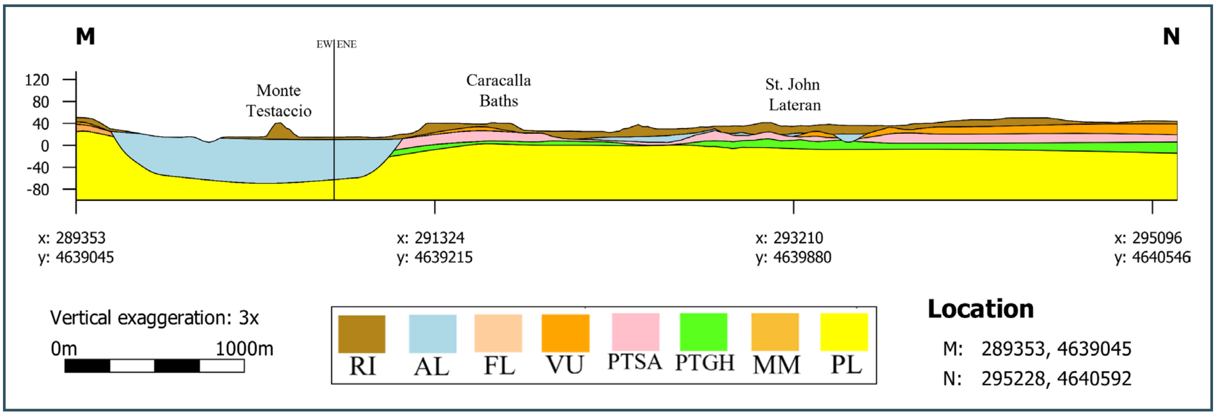
M
N
120
80
40
0
-40
-80
Monte Testaccio
Caracalla Baths
St. John Lateran
x: 289353 y: 4639045
x: 291324 y: 4639215
x: 293210 y: 4639880
x: 295096 y: 4640546
Vertical exaggeration: 3x
0m
1000m
RI AL FL VU PTSA PTGH MM PL
Location
M: 289353, 4639045
N: 295228, 4640592

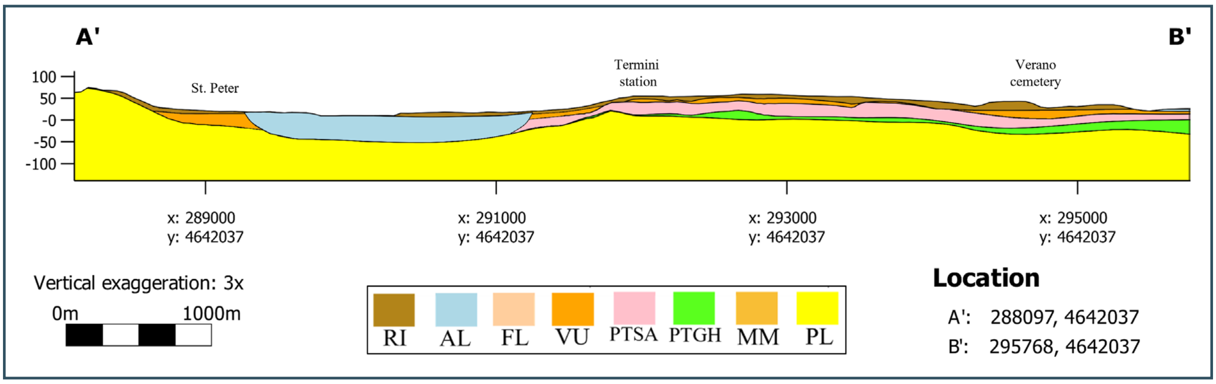
A'
B'
100
50
-0
-50
-100
St. Peter
Termini station
Verano cemetery
x: 289000 y: 4642037
x: 291000 y: 4642037
x: 293000 y: 4642037
x: 295000 y: 4642037
Vertical exaggeration: 3x
0m
1000m
RI AL FL VU PTSA PTGH MM PL
Location
A': 288097, 4642037
B': 295768, 4642037

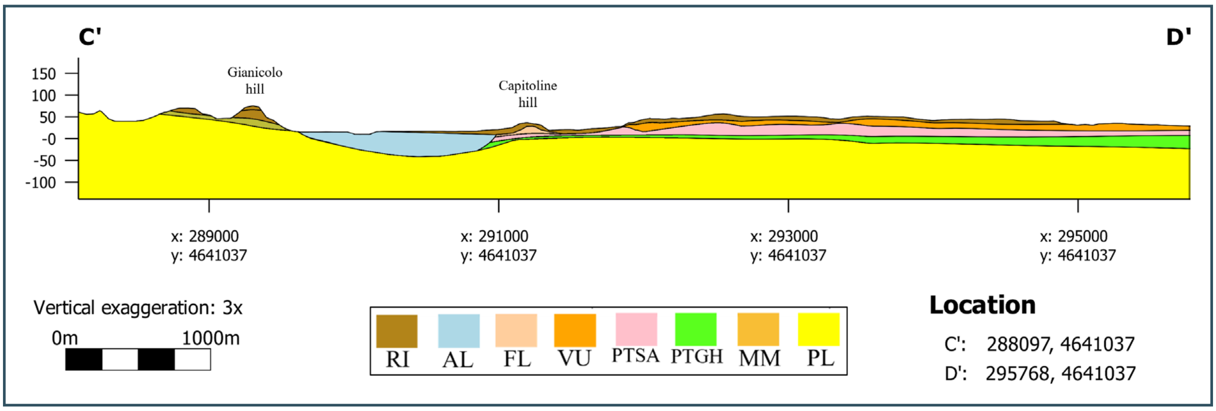
C'
D'
150
100
50
-0
-50
-100
Gianicolo hill
Capitoline hill
x: 289000 y: 4641037
x: 291000 y: 4641037
x: 293000 y: 4641037
x: 295000 y: 4641037
Vertical exaggeration: 3x
0m
1000m
RI AL FL VU PTSA PTGH MM PL
Location
C': 288097, 4641037
D': 295768, 4641037

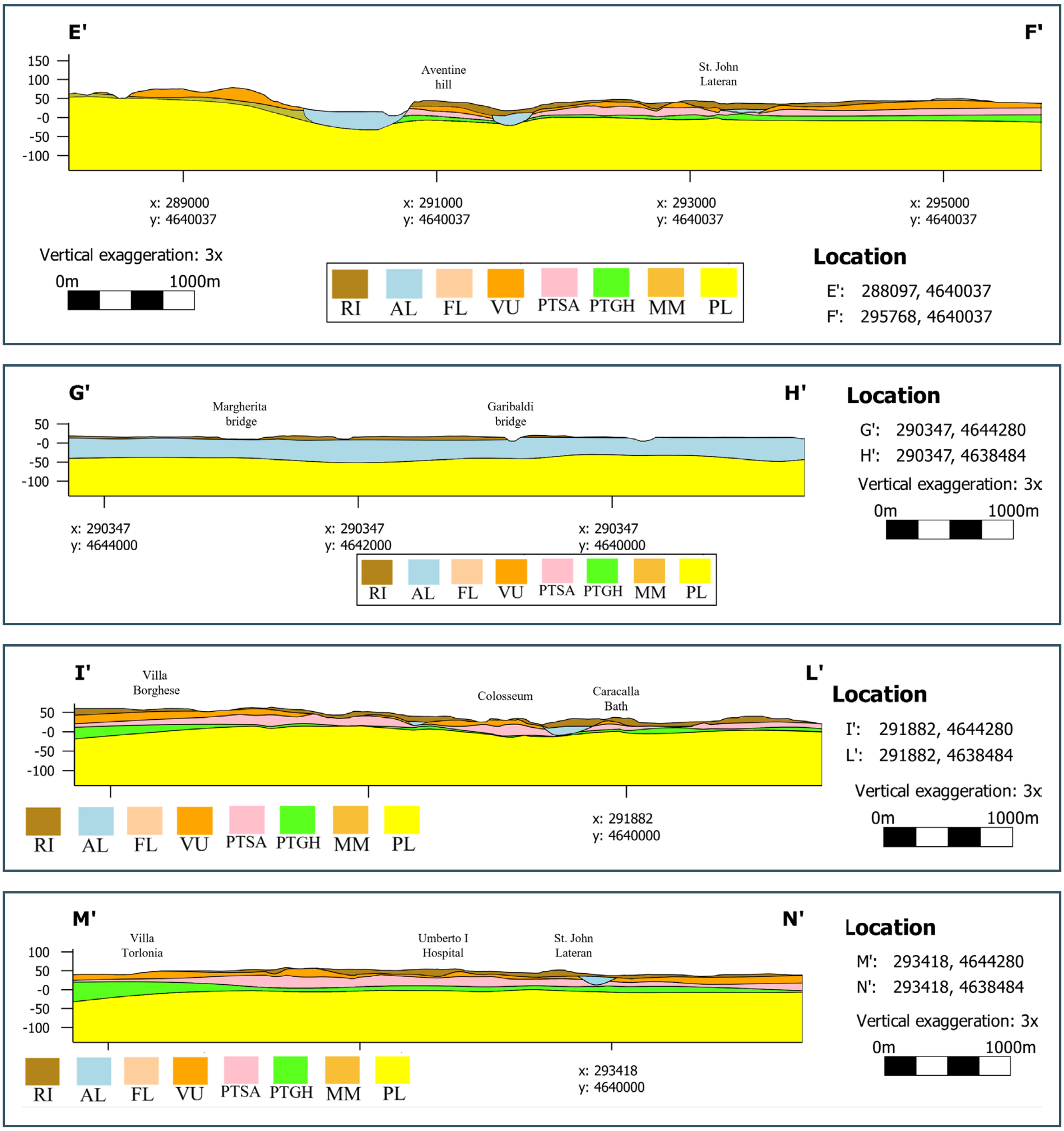
E'
F'
150
100
50
-0
-50
-100
Aventine hill
St. John Lateran
x: 289000 y: 4640037
x: 291000 y: 4640037
x: 293000 y: 4640037
x: 295000 y: 4640037
Vertical exaggeration: 3x
0m 1000m
RI AL FL VU PTSA PTGH MM PL
Location
E': 288097, 4640037
F': 295768, 4640037
G'
H'
50
-0
-50
-100
Margherita bridge
Garibaldi bridge
x: 290347 y: 4644000
x: 290347 y: 4642000
x: 290347 y: 4640000
RI AL FL VU PTSA PTGH MM PL
Location
G': 290347, 4644280
H': 290347, 4638484
Vertical exaggeration: 3x
0m 1000m
I'
L'
Villa Borghese
Colosseum
Caracalla Bath
50
-0
-50
-100
RI AL FL VU PTSA PTGH MM PL
x: 291882 y: 4640000
Location
I': 291882, 4644280
L': 291882, 4638484
Vertical exaggeration: 3x
0m 1000m
M'
N'
Villa Torlonia
Umberto I Hospital
St. John Lateran
100
50
-0
-50
-100
RI AL FL VU PTSA PTGH MM PL
x: 293418 y: 4640000
Location
M': 293418, 4644280
N': 293418, 4638484
Vertical exaggeration: 3x
0m 1000m

Appendix B. Thickness maps

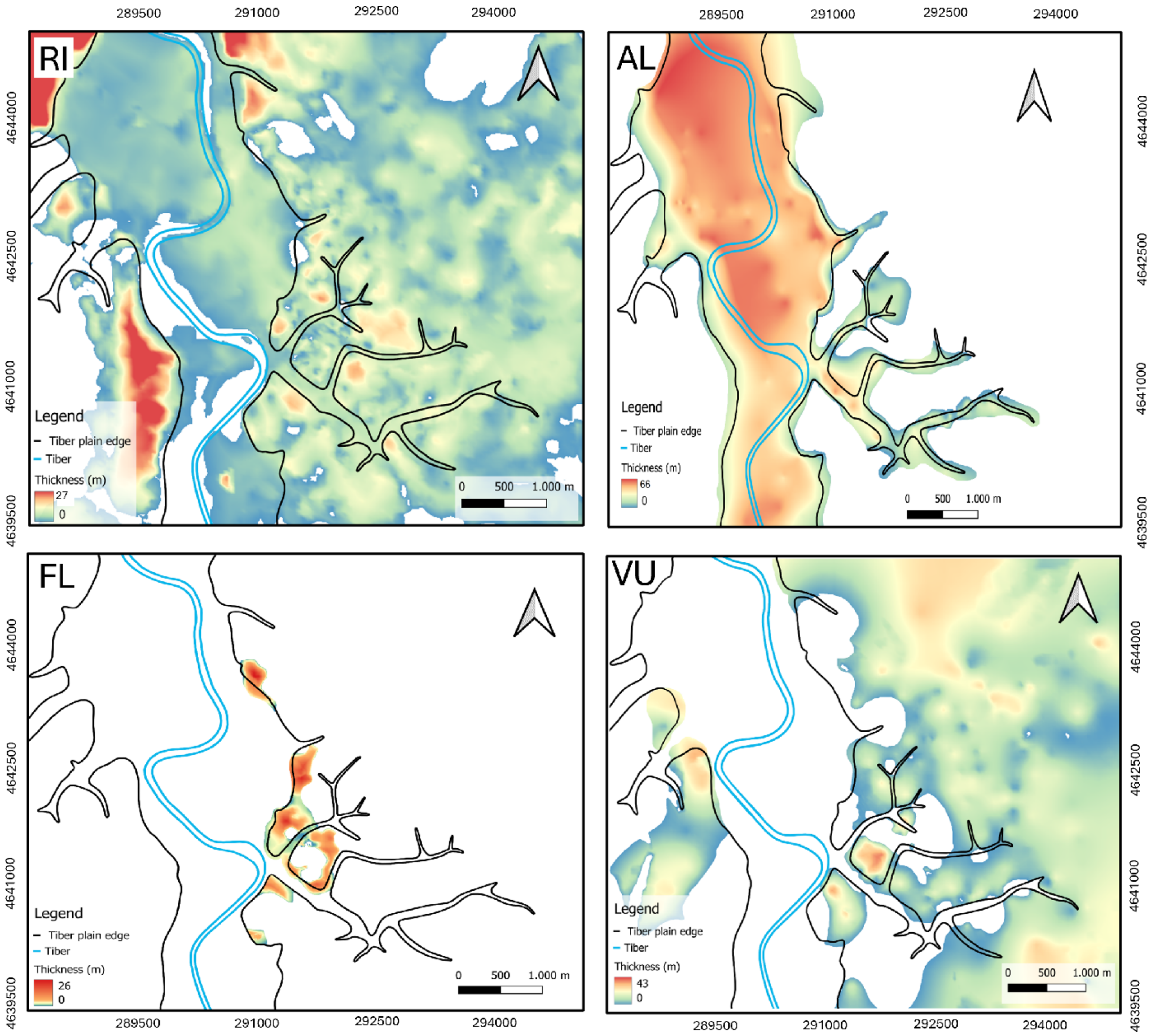

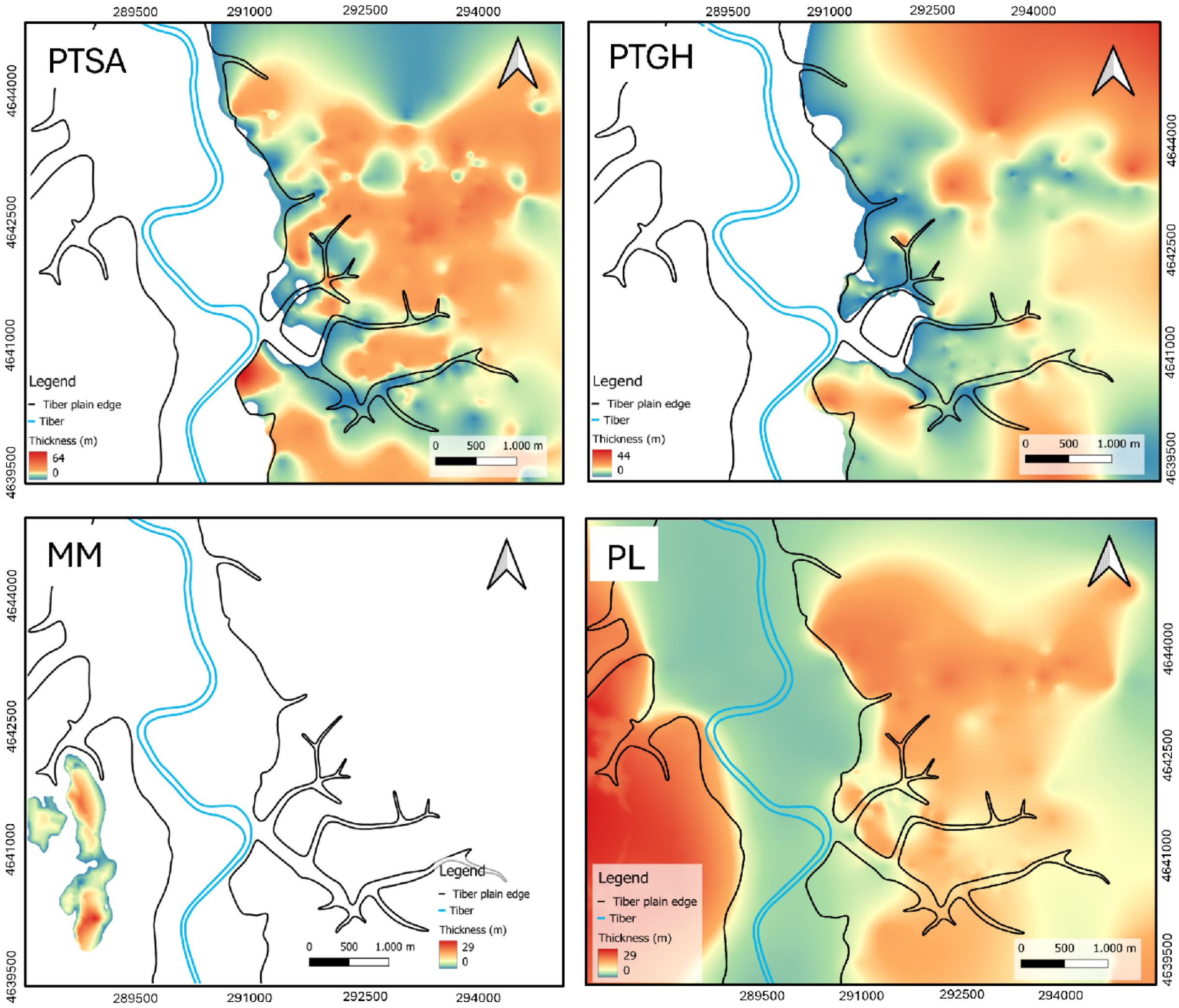

***CORRESPONDING AUTHOR: Daniele SILVESTRI**,
University of Siena, Department of Physical Sciences, Earth and Environment, Siena, Italy
e-mail: daniele.silvestri@unisi.it